

## Chapter 2

# Intra-oceanic Subduction Zones

T.V. Gerya

### 2.1 Introduction

According to the common definition, intra-oceanic subduction brings oceanic slabs under the overriding plates of oceanic origin. As a consequence oceanic magmatic arcs are formed worldwide (Fig. 2.1) with typical examples such as the Izu-Bonin-Mariana arc, the Tonga-Kermadec arc, the Vanuatu arc, the Solomon arc, the New Britain arc, the western part of the Aleutian arc, the South Sandwich arc and the Lesser Antilles arc (Leat and Larter 2003). Intra-oceanic subduction zones comprise around 17,000 km, or nearly 40%, of the subduction margins of the Earth (Leat and Larter 2003). Indeed, intra-oceanic arcs are less well studied than continental arcs since their major parts are often located below sea level, sometimes with only the tops of the largest volcanoes forming islands. Intra-oceanic subduction zones are sites of intense magmatic and seismic activities as well as metamorphic and tectonic processes shaping out arc compositions and structures. During an ocean closure (e.g., Collins 2003) such arcs may collide with continental margins creating distinct structural and compositional record in continental orogens (such as in Himalaya, Burg 2011) which makes them of particular interest for the present book.

Several years ago Leat and Larter (2003) published a comprehensive review on intra-oceanic subduction systems. The review focused on tectonic and magmatic processes in intra-oceanic arcs and was mainly

based on observational constraints. In addition, Schellart et al. (2007) compiled detailed nomenclature and taxonomy of Subduction zones worldwide. The following major characteristics of intra-oceanic subduction zones can be summarized (Leat and Larter 2003; Schellart et al. 2007 and references therein)

- *Convergence rates* vary from ca 2 cm/yr in the Lesser Antilles arc to 24 cm/yr in the northern part of the Tonga arc, the highest subduction rates on Earth. Typical rates are in the range 5–13 cm/yr. Intra-arc variations are almost as large as inter-arc ones.
- *Ages of subducting slabs* range from ca 150 Ma (Pacific Plate subducting beneath the Mariana arc) to close to zero age (along part of the Solomon arc). Along-arc variations in slab ages are typically not large ( $\pm 10$  Ma). There are indeed large variations in the topography of the subducting plates (up to 5 km, Fig. 2.1): some are relatively smooth, some contain ridges and seamounts that affect subduction and arc tectonics.
- *Sediment thicknesses* are notably variable (from 70 m to >6 km, typically 150–650 m). Sediment cover is commonly thinner over basement highs. Variations in thickness and composition of subducted sediments are probably greatest where arcs are close to, or cut across, ocean–continent boundaries.
- *Accretion v. non-accretion*. Most modern intra-oceanic arcs are non-accreting, i.e. there is little or no net accumulation of off-scraped sediment forming accretionary complexes. In other words, all the sediments arriving at the trenches are subducted (over a period) into the mantle. The two exceptions are the Lesser Antilles and Aleutian arcs, both of which have relatively high sediment inputs and where accretionary complexes have formed.

---

T.V. Gerya

Geophysical Fluid Dynamics Group, Department of Earth Sciences, Institute of Geophysics, Swiss Federal Institute of Technology (ETH-Zurich), Sonneggstrasse, 5, 8092 Zurich, Switzerland

e-mail: taras.gerya@erdw.ethz.ch

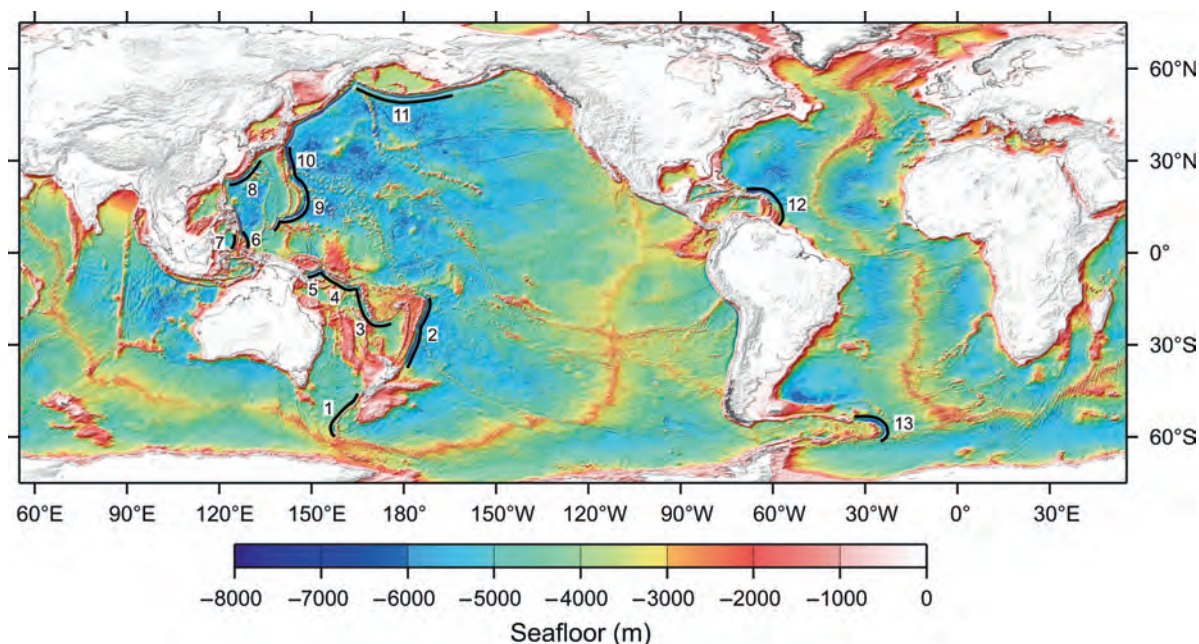


**Fig. 2.1** Location of modern intra-oceanic subduction zones. The trenches of these subduction systems are indicated by heavy black lines, and identified by numbers that correspond to those of Leat and Larter (2003): 1 – MacQuarie; 2 – Tonga-Kerma-

dec; 3 – Vanuatu (New Hebrides); 4 – Solomon; 5 – New Britain; 6 – Halmahara; 7 – Sangihe; 8 – Ryuku; 9 – Mariana; 10 – Izu-Bonin (Ogasawara); 11 – Aleutian; 12 – Lesser Antilles; 13 – South Sandwich

- 70 • *Back-arc extension.* Most of the arcs have closely  
71 associated back-arc rifts. Only the Solomon and  
72 Aleutian arcs are exceptions in having no apparent  
73 back-arc extension. In most cases, the back-arc  
74 extension takes the form of well-organized seafloor  
75 spreading for at least part of the length of the back-  
76 arc. Such spreading appears to follow arc extension  
77 and rifting in at least some cases.
- 78 • *Arc thicknesses* depend on arc maturity, tectonic  
79 extension or shortening, and the thickness of pre-  
80 arc basement. Only approximately, therefore, is it  
81 true to say that the thin crusts (e.g. of the South  
82 Sandwich and Izu-Osgaswara) arcs represent arcs  
83 in the relatively early stages of development,  
84 whereas arcs with thicker crusts are more mature  
85 (e.g. the Lesser Antilles and Aleutian arcs).
- 86 • *Pre-arc basements* of the arcs are very variable.  
87 Only one intra-oceanic arc (the Aleutian arc) is  
88 built on normal ocean crust. The others are built  
89 on basements comprising a range of oceanic lithol-  
90 ogies, including ocean crust formed at back-arc  
91 spreading centres, earlier intra-oceanic arcs, accre-  
92 tionary complexes and oceanic plateaux. This also

points out toward complexity of intraoceanic sub- 93  
duction (re)initiation scenarios. 94

In the recent years significant new literature on 95  
intra-oceanic subduction appeared (in particular, on 96  
high-resolution seismic studies of arc structures and 97  
on numerical modeling of intra-oceanic subduction) 98  
that should be added to the state-of-the-art knowledge 99  
which is one of the reasons for writing this chapter. 100  
Also, taking into account that the present volume 101  
mainly concentrates on arc collision processes I will 102  
focus the review on relatively shallow portions of 103  
intraoceanic subduction-arc system from which the 104  
record can be preserved in the resulting collision 105  
zones (e.g. Burg 2011). The following major issues 106  
will be discussed in the review 107

- Initiation of intra-oceanic subduction 108
- Internal structure and composition of arcs 109
- Subduction channel processes 110
- Dynamics of crustal growth 111
- Geochemistry of intra-oceanic arcs 112

In order to keep a cross-disciplinary spirit of mod- 113  
ern intra-oceanic subduction studies often combining 114

115 observational constrains with results of numerical  
 116 geodynamic modelling the later will be used here  
 117 for visualizing various subduction-related processes  
 118 instead of more traditional hand-drawn cartoons.

## 119 2.2 Initiation of Intra-oceanic 120 Subduction

121 It is yet not entirely clear how subduction in general  
 122 and intraoceanic subduction in particular is initiated.  
 123 The gravitational instability of an old oceanic plate is  
 124 believed to be the main reason for subduction (Vlaar  
 125 and Wortel 1976; Davies 1999). Oceanic lithosphere  
 126 becomes denser than the underlying asthenosphere  
 127 within 10–50 Ma after it forms in a mid-ocean ridge  
 128 due to the cooling from the surface (Oxburg and  
 129 Parmentier 1977; Cloos 1993; Afonso et al. 2007,  
 130 2008). However, despite the favourable gravitational  
 131 instability and ridge-push, the bending and shear resis-  
 132 tance of the lithosphere prevent subduction from arising  
 133 spontaneously (McKenzie 1977). Consequently,  
 134 the following question arises: what forces can trigger  
 135 subduction (besides the negative buoyancy and ridge-  
 136 push)? At least 12 hypotheses have been proposed to  
 137 answer this question:

- 138 1. Plate rupture within an oceanic plate or at a  
 139 passive margin (e.g. McKenzie 1977; Dickinson  
 140 and Seely 1979; Mitchell 1984; Müeller and  
 141 Phillips 1991).
- 142 2. Reversal of the polarity of an existing subduction  
 143 zone (e.g. Mitchell 1984).
- 144 3. Change of transform faults into trenches (e.g.  
 145 Uyeda and Ben-Avraham 1972; Hilde et al. 1976;  
 146 Karson and Dewey 1978; Casey and Dewey 1984).
- 147 4. Sediment or other topographic loading at conti-  
 148 nental/arc margins (e.g. Dewey 1969; Fyfe and  
 149 Leonardos 1977; Karig 1982; Cloetingh et al.  
 150 1982; Erickson 1993; Pascal and Cloetingh 2009).
- 151 5. Forced convergence at oceanic fracture zones  
 152 (e.g. Müeller and Phillips 1991; Toth and Gurnis  
 153 1998; Doin and Henry 2001; Hall et al. 2003;  
 154 Gurnis et al. 2004).
- 155 6. Spontaneous initiation of retreating subduction  
 156 (Fig. 2.2) due to a lateral thermal buoyancy con-  
 157 trast at oceanic fracture zones separating oceanic

- plates of contrasting ages (e.g. Gerya et al. 2008; 158  
 Nikolaeva et al. 2008; Zhu et al. 2008). 159 AU1
7. Tensile decoupling of the continental and oceanic 160  
 lithosphere due to rifting (Kemp and Stevenson 161  
 1996). 162
8. Rayleigh-Taylor instability due to a lateral com- 163  
 positional buoyancy contrast within the litho- 164  
 sphere (Niu et al. 2003). 165
9. Addition of water into the lithosphere (Regenauer- 166  
 Lieb et al. 2001; Van der Lee et al. 2008). 167
10. Spontaneous thrusting (Fig. 2.3) of the buoyant 168  
 continental/arc crust over the oceanic plate (Mart 169  
 et al. 2005; Nikolaeva et al. 2010; Goren et al. 170  
 2008). 171
11. Small-scale convection in the sub-lithospheric 172  
 mantle (Solomatov 2004). 173
12. Interaction of thermal-chemical plumes with the 174  
 lithosphere (Ueda et al. 2008). 175

In the recent review by Stern (2004 and references 176  
 therein) two major types of subduction initiation sce- 177  
 narios applicable to intraoceanic subduction are pro- 178  
 posed based on both theoretical considerations and 179  
 natural data: induced and spontaneous. Induced sub- 180  
 duction nucleation may follow continuation of plate 181  
 convergence after jamming of a previously active sub- 182  
 duction zone (e.g. due to arrival of a buoyant crust to 183  
 the trench). This produces regional compression, uplift 184  
 and underthrusting that may yield a new subduction 185  
 zone in a different place. Two subtypes of induced 186  
 initiation, transference and polarity reversal, are dis- 187  
 tinguished (Stern 2004 and references therein). Trans- 188  
 ference initiation moves the new subduction zone 189  
 outboard of the failed one. The Mussau Trench and 190  
 the continuing development of a plate boundary SW of 191  
 India in response to Indo–Asian collision are the best 192  
 Cenozoic examples of transference initiation pro- 193  
 cesses (Stern 2004 and references therein). Polarity 194  
 reversal initiation also follows collision, but continued 195  
 convergence in this case results in a new subduction 196  
 zone forming behind the magmatic arc; the response of 197  
 the Solomon convergent margin following collision 198  
 with the Ontong Java Plateau (Stern 2004 and refer- 199  
 ences therein) and dramatic reorganization of the tec- 200  
 tonic plate boundary in the New Hebrides region 201  
 (Pysklywec et al. 2003 and references therein) are 202  
 suggested to be the examples of this mode. 203

Spontaneous nucleation results from inherent gravi- 204  
 tational instability of sufficiently old oceanic lithosphere 205

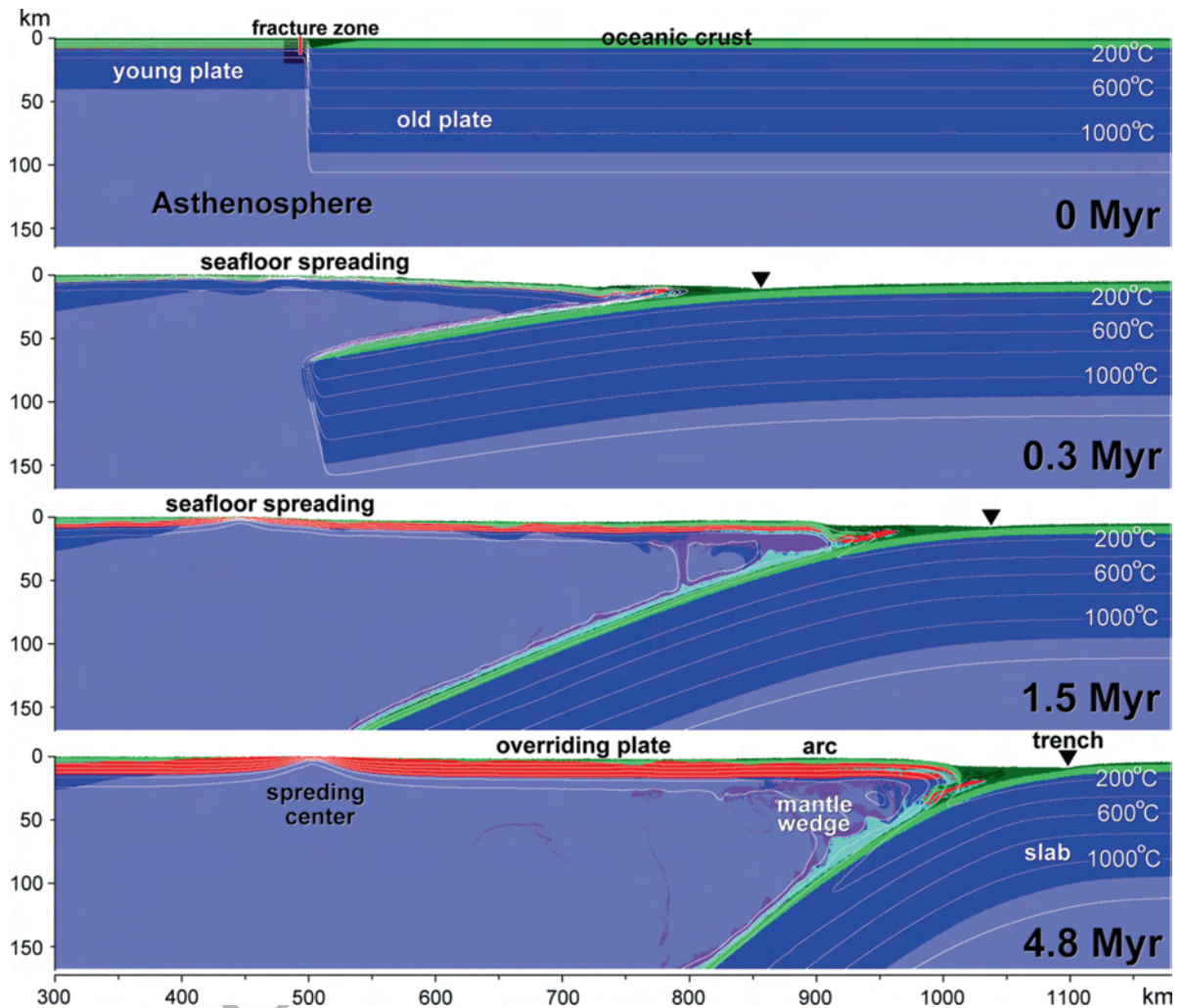


**Fig. 2.2** Dynamics of spontaneous initiation of retreating subduction at a transform/fracture zone separating oceanic plates of contrasting ages. Results from 2D numerical experiments by Gerya et al. (2008)

206 compared to the underlying mantle, which is also the  
 207 main reason for operating of the modern regime of  
 208 plate tectonics. It is widely accepted (e.g. Stern 2004  
 209 and references therein) that intra-oceanic subduction  
 210 can initiate spontaneously either at a transform/fracture  
 211 zone (Fig. 2.2) or at a passive continental/arc margin  
 212 (Fig. 2.3), in a fashion similar to lithospheric delami-  
 213 nation. According to the theoretical prediction (e.g.  
 214 Stern 2004) and numerical modeling results (e.g.  
 215 Gerya et al. 2008; Nikolaeva et al. 2008; Zhu et al.  
 216 2009) spontaneous initiation across a fracture zone  
 217 separating oceanic plates of contrasting ages associ-  
 218 ates with an intense seafloor spreading (Fig. 2.2,  
 219 0.3–1.5 Myr), as asthenosphere wells up to replace

220 sunken lithosphere of the older plate. This is the pre- 220  
 221 sumable origin of most boninites and ophiolites (Stern 221  
 222 2004 and references therein). Such initiation process 222  
 223 assumed to have produced new subduction zones along 223  
 224 the western edge of the Pacific plate during the Eocene 224  
 225 (Stern 2004 and references therein). Development of 225  
 226 self-sustaining one-sided subduction is marked by the 226  
 227 beginning of down-dip slab motion, formation of the 227  
 228 mantle wedge and appearance of the magmatic arc at 228  
 229 100–200 km distance from the retreating trench 229  
 230 (Fig. 2.2). 230

231 Passive continental/arc margin collapse (Fig. 2.3) is 231  
 232 driven by the geometry of the margin, where relatively 232  
 233 thick (20–35 km) low-density continental/arc crust is 233

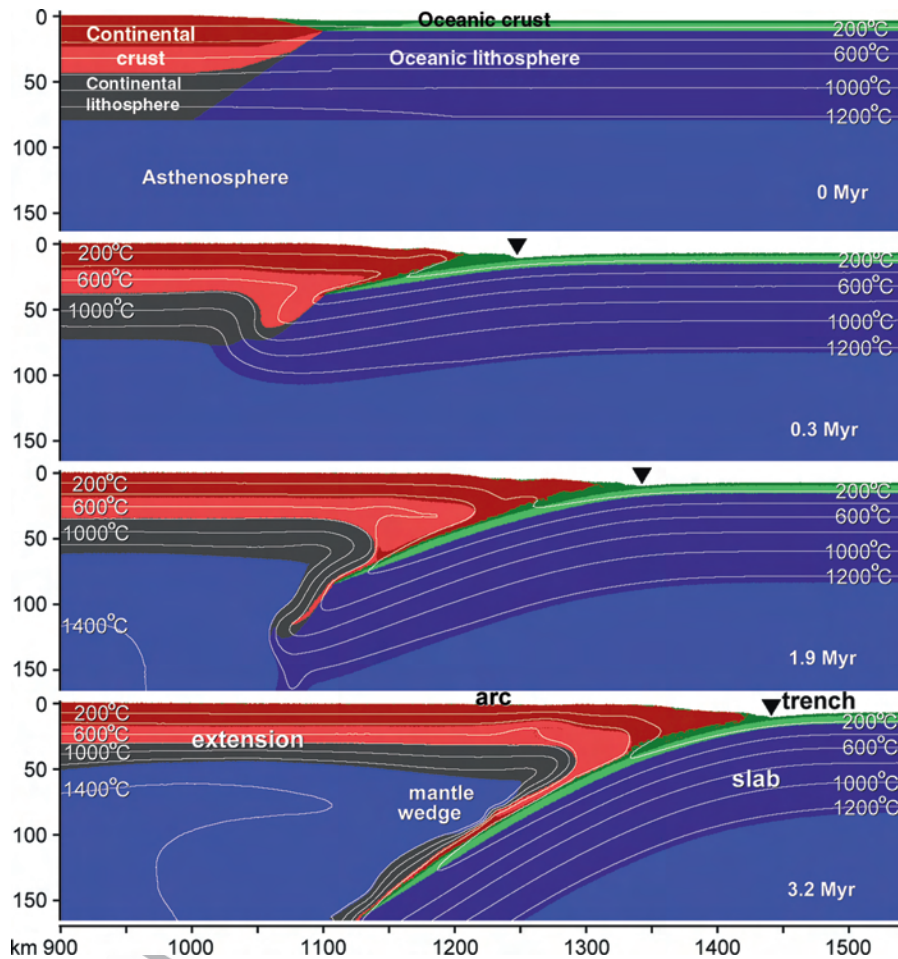


**Fig. 2.3** Dynamics of spontaneous subduction initiation at a passive continental/arc margin. Results from 2D numerical experiments by Nikolaeva et al. (2010)

234 bounded laterally by significantly more dense oceanic  
 235 lithosphere. When during the margin evolution forces  
 236 generated from this lateral density contrast become big  
 237 enough to overcome the continental/arc crust strength  
 238 then this crust starts to creep over the oceanic one  
 239 (Fig. 2.3, 0.3 Myr). This causes deflection of the oceanic  
 240 lithosphere (Fig. 2.3, 0.3 Myr) and may actually lead to  
 241 its delamination from the continental/arc lithosphere  
 242 (Fig. 2.3, 0.3–1.9 Myr) thus triggering retreating sub-  
 243 duction process (Fig. 2.3, 1.9–3.2 Myr). This type of  
 244 subduction nucleation has been successfully modelled  
 245 with both analogue (Mart et al. 2005; Goren et al. 2008)  
 246 and numerical (Nikolaeva et al. 2010) techniques. No  
 247 undeniable modern example of such ongoing subduc-  
 248 tion initiation is yet known: a possible recent exception  
 249 is suggestion for subduction/overthrusting initiation at

the eastern Brazilian margin (Marques et al. 2008). 250  
 Indeed, Goren et al. (2008) speculated that such type 251  
 of initiation was relevant in the past for two active 252  
 intra-oceanic subduction systems in which Atlantic 253  
 lithosphere is being subducted: the Lesser-Antilles 254  
 and the South Sandwich subduction systems. Also, 255  
 Masson et al. (1994) and Alvarez-Marron et al. 256  
 (1996, 1997) argued that an arrested subduction zone 257  
 nucleation can be distinguished in the North Iberian 258  
 Margin based on structural and seismic data. 259

Both spontaneous and induced subduction initia- 260  
 tion can be potentially distinguished by the record 261  
 left on the upper plates: induced nucleation begins 262  
 with strong compression and uplift, whereas sponta- 263  
 neous one begins with rifting and seafloor spreading 264  
 (Stern et al., 2004). 265

## 2.3 Internal Structure of Intra-oceanic Arcs

Internal structure and compositions of intra-oceanic arcs are strongly variable depending on both the pre-existing plate structure and on the dynamics of subduction and associated crustal growth (e.g. Leat and Larter 2003). In addition, deep parts of the arcs are mainly reconstructed based on seismic data and fragmentary records left in orogens after arc-continent collisions, which creates further uncertainties for interpretations of intra-oceanic arc structures. As was indicated by Tatsumi and Stern (2006) understanding how continental crust forms at intra-oceanic arcs requires knowledge of how intra-oceanic arcs form and mature with key questions being:

1. What is the nature of the crust and mantle in the region prior to the beginning of subduction?
2. How does subduction initiate and initial arc crust form?
3. How do the middle and lower arc crusts evolve?

4. What are the spatial changes of arc magma and crust compositions of the entire arc?

In this respect, in addition to robust natural data, realistic self-consistent numerical modelling of subduction and associated crustal growth (e.g., Nikolaeva et al. 2008; Kimura et al. 2009; Sizova et al. 2009; Gerya and Meilick 2010) can complement the interpretations of details and variability in arc structures. Figure 2.4 shows a schematic cross-section across a mature intra-oceanic arc corresponding to the retreating subduction regime. The cross-section is based on recent results of numerical petrological-thermomechanical modelling (Gerya and Meilick 2010). The following major structural components of the arc can be distinguished based on this scheme and natural data: (a) accretion prism (if present), (b) pre-arc basement (c) serpentinized fore-arc including subduction channel composed of tectonic melange, (d) magmatic crust, (e) sub-arc lithosphere (cumulates?, replacive rocks?), (f) back-arc region with new oceanic floor and a spreading center and (g) paleo-arc (in the rear part

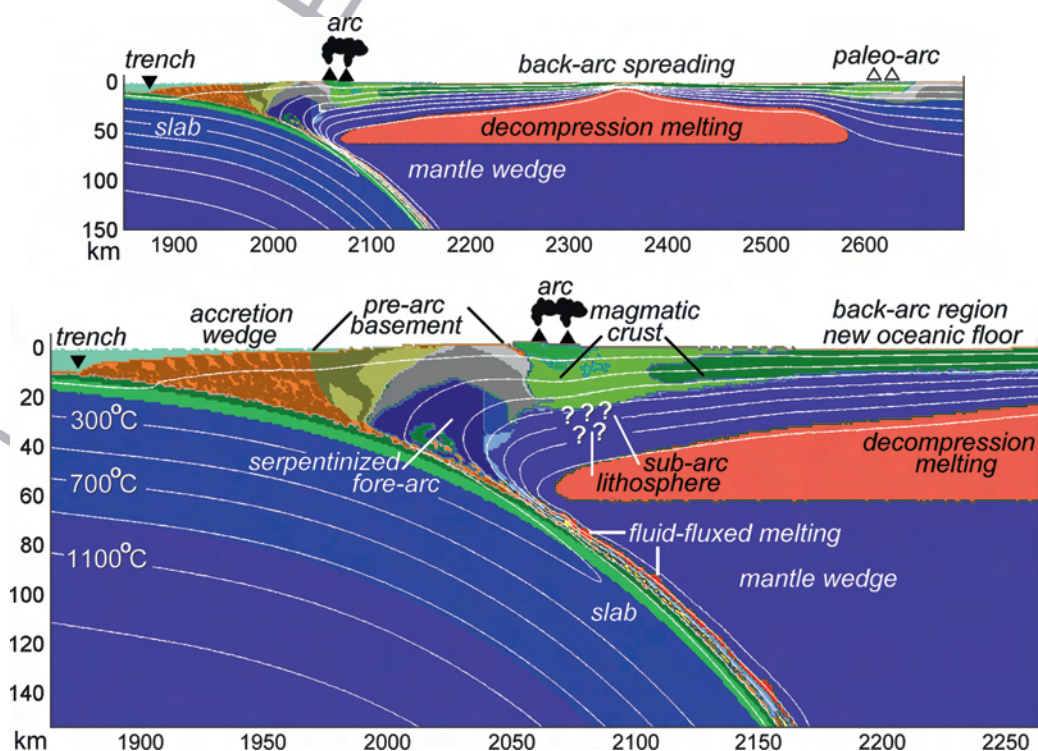


**Fig. 2.4** Schematic cross-section of an intra-oceanic arc associated with retreating subduction. Results from 2D numerical experiments by Gerya and Meilick (2010)

of the back-arc spreading domain). Obviously this structure is non-unique and significant variations can be expected in both nature (e.g. Tatsumi and Stern 2006; Takahashi et al. 2007, 2009; Kodaira et al. 2006, 2007, 2008) and models (e.g. Nikolaeva et al. 2008; Sizova et al. 2009; Gerya and Meilick 2010), depending on arc history, subduction dynamics and sub-arc variations in melt production intensity, distribution and evolution (e.g. Tamura 1994; Tamura et al. 2002; Honda et al. 2007; Zhu et al. 2009).

Recently new high-resolution data (see Calvert 2011) were obtained concerning seismic structure of the arc crust in Izu-Bonin-Mariana system (e.g. Takahashi et al. 2007, 2009; Kodaira et al. 2006, 2007, 2008). These data suggest that lateral variations in crustal thickness, structure and composition occur both along and across intra-oceanic arcs (e.g. Figs. 2-4, 2-6 in Calvert 2011; Kodaira et al. 2006; Takahashi et al. 2009). Such variations are interpreted as being the results of laterally and temporally variable magmatic addition and multiple episodes of fore-arc, intra-arc and back-arc extension (e.g. Takahashi et al. 2007, 2009; Kodaira et al. 2006, 2007, 2008). Seismic models demonstrate notable velocity variations (Fig. 2-6 in Calvert 2011) within the arc middle and lower crusts, which are interpreted to be respectively of intermediate to felsic and mafic compositions (e.g. Takahashi et al. 2007). In the regions of the maximal thickness (around 20 km, Fig. 2-6 in Calvert 2011) the oceanic-island-arc crust is composed of a volcanic-sedimentary upper crust with velocity of less than 6 km/s, a middle crust with velocity of  $\sim 6$  km/s, laterally heterogeneous lower crust with velocities of  $\sim 7$  km/s, and unusually low mantle velocities (Takahashi et al. 2009; also see crust-mantle transition layer in Fig. 2-6b, c in Calvert 2011). Petrologic modeling of Takahashi et al. (2007) suggests that the volume of the lower crust, presumably composed of restites and olivine cumulates remained after the extraction of the middle crust, should be significantly larger than is observed on the seismic cross-sections. Therefore, such mafic-ultramafic part of the lower crust (if at all present in the arcs, e.g. Jagoutz et al. 2006) should have seismic properties similar to the mantle ones and consequently look seismically as a part of the mantle lithosphere.

There are notable uncertainties in interpreting seismic structures of intra-oceanic arcs, which are related to current uncertainties in understanding melt differ-

entiation processes under the arcs. As summarised by Leat and Larter (2003) the major element composition of magmas feeding arcs from the mantle has been and remain (e.g. Jagoutz et al. 2006) a subject of debate, particularly regarding the Mg and Al contents of primary magmas. Mafic compositions in arcs have variable MgO content, but with a clear cut-off at about 8 wt% MgO or even less (in the case of mature arcs). High-MgO, primitive non-cumulate magmas have indeed been identified in many arcs, but they are always volumetrically very minor (Davidson 1996). One question is, therefore, whether the MgO cut-off point represents composition of the mantle-derived parental magmas, or whether the mantle-derived parental magmas are significantly more MgO-rich ( $>10\%$  MgO), but are normally unable to reach the surface and erupt. It has been argued that they have difficulty in traversing the crust without encountering magma chambers because of their relatively high density (Smith et al. 1997; Leat et al. 2002). In addition, as argued by Pichavant and Macdonald (2003) only the most water-poor primitive magmas are able to traverse the crust without adiabatically freezing.

It should, however, be mentioned that the above explanations are not fully satisfactory in explaining the "MgO-paradox". First, as has recently been demonstrated numerically (Gerya and Burg 2007; Burg et al. 2009) local density contrast between rising dense magmas and surrounding crustal rocks plays only a secondary role compared the rheology of the crust. According to the numerical results, in case of relatively strong lower crust even very dense ultramafic magmas can easily reach the surface given that they are generated below a sufficiently dense and thick mantle lithosphere. Second, when differentiation of the parental high-MgO mantle-derived magma takes place inside the arc crust, significant volumes of high-MgO cumulates should be produced. Fractionation models indicate that 15–35% crystallization is necessary to lower the MgO content adequately (e.g., Conrad and Kay 1984). Such cumulates should either (1) form a major component below the seismic Moho (e.g. Kay and Kay 1985; Müntener et al. 2001; Takahashi et al. 2007) or (2) delaminate and sink back into the mantle (e.g., Kay and Kay 1991, 1993; Jull and Kelemen 2001). The delamination theory is presently favoured based on the lack of appropriate upper mantle rocks brought to the surface in continental regions

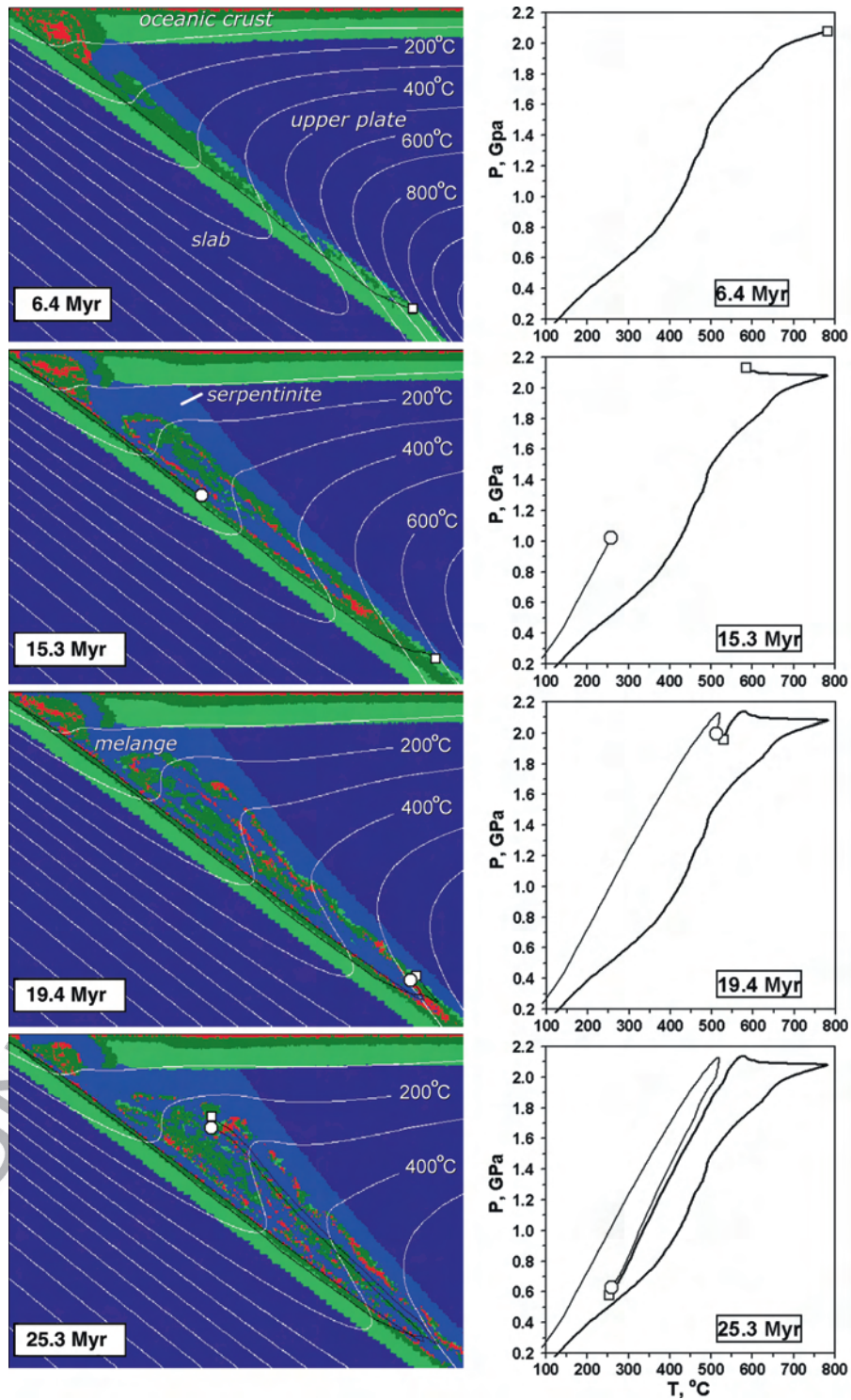


**Fig. 2.5** Spontaneous development of weak serpentinized subduction channel during intra-oceanic subduction. Left column – development of the lithological field and isotherms (white lines, °C). Right column – development of P–T paths for two rock

fragments (see open circle and open rectangle in the left column). Results from 2D numerical modelling by Gerya et al. (2002)

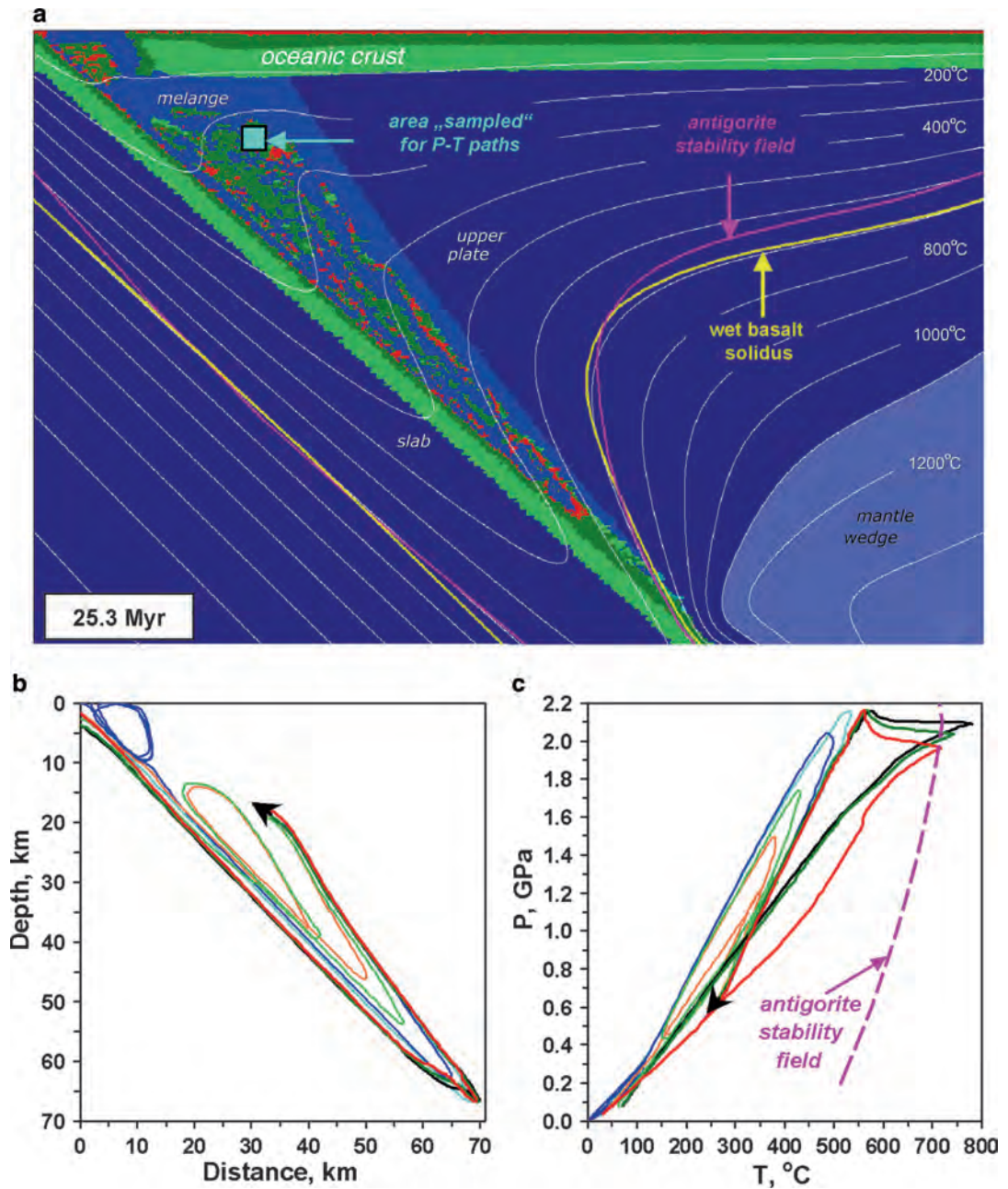


**Fig. 2.6** Serpentinite melange (a) forming in the spontaneously evolving subduction channel (Fig. 2.6) and characteristic spatial trajectories (b) and P-T paths (c) of crustal rocks composing the

melange. Results from 2D numerical modelling by Gerya et al. (2002)

406 (e.g. Rudnick and Gao 2003), the absence of primitive  
 407 cumulate rocks in the exposed Talkeetna paleo-island  
 408 arc crust section (Kelemen et al. 2003) and evidence  
 409 for active foundering of the lower continental crust

below the southern Sierra Nevada, California (Zandt 410  
 et al. 2004; Boyd et al. 2004). 411

An alternative explanation of magma differentia- 412  
 tion processes in the arcs has recently been proposed 413

414 by Jagoutz et al. (2007) based on geochemical  
 415 data from the Kohistan paleo-arc in NW Pakistan.  
 416 According to this hypothesis the melt rising through  
 417 the Moho boundary of an arc has already a low-MgO  
 418 basaltic–andesitic composition, while the primary  
 419 magma generated in the mantle wedge is a high-MgO  
 420 primitive basaltic liquid. Fractionation of the mantle-  
 421 derived melt takes place in the mantle lithosphere  
 422 within km-scaled isolated conduits (replacive chan-  
 423 nels). The dunitic ultramafic bodies found in the  
 424 lowermost section of the Kohistan paleo-arc are inter-  
 425 preted as remnants of such melt channels through  
 426 which the low-MgO (i.e. differentiated) lower-crustal  
 427 intrusive mafic sequence was fed. As suggested by  
 428 Jagoutz et al. (2007) such differentiation within the  
 429 upper mantle is an important lower crust-forming pro-  
 430 cess which can also explain the absence of high-MgO  
 431 cumulates in the lower crust of exposed island arcs  
 432 (e.g., Kelemen et al. 2003).

## 433 2.4 Subduction Channel Processes

434 Subduction channel development is an important  
 435 component of intra-oceanic arc evolution (Fig. 2.4).  
 436 Processes taking place in the subduction channel lives  
 437 notable and directly accessible record at the surface in  
 438 form of exhumed high- and ultrahigh-pressure rocks  
 439 complexes (e.g., Ernst 1977; Cloos 1982; Shreve and  
 440 Cloos 1986; Hermann et al. 2000; Abbott et al. 2006;  
 441 Federico et al. 2007; Krebs et al. 2008). Subduction  
 442 channel processes may also contribute to a magmatic  
 443 record through deep subduction and melting of  
 444 hydrated rock mélanges formed in the channel (e.g.,  
 445 Gerya and Yuen 2003; Gerya et al. 2006; Castro and  
 446 Gerya 2008; Zhu et al. 2009).

447 It is widely accepted that the deep burial of high  
 448 pressure metamorphic rocks in intra-oceanic settings  
 449 is due to subduction of these rocks with the downgoing  
 450 slab. However, the mechanisms of their exhumation  
 451 remain subject of discussion and several models  
 452 have been proposed (e.g., Cloos 1982; Platt 1993;  
 453 Maruyama et al. 1996; Ring et al. 1999). According  
 454 to the most popular corner flow model (Hsu 1971;  
 455 Cloos 1982; Cloos and Shreve 1988a, b; Shreve and  
 456 Cloos 1986; Gerya et al. 2002), exhumation of high-  
 457 pressure metamorphic crustal slices at rates on the

order of the plate velocity is driven by forced flow in  
 a wedge-shaped subduction channel.

Gerya et al. (2002) investigated numerically the  
 self-organizing evolution of the accretionary wedge  
 and the subduction channel during intra-oceanic sub-  
 duction (Fig. 2.5). In this model the geometry of the  
 accretionary wedge and the subduction channel are  
 neither prescribed nor assumed to represent a steady  
 state. Instead, the system is free to evolve, starting  
 from an imposed early stage of subduction, being  
 controlled by the progressive modification of the  
 thermal, petrological, and rheological structure of the  
 subduction zone. In this evolution, upward migration  
 of the aqueous fluid released from the subducting  
 slab and progressive hydration of the mantle wedge  
 play a dominant role. The following conclusions  
 have been made based on numerical results (Gerya  
 et al. 2002):

- Burial and exhumation of high-pressure metamorphic rocks in subduction zones are likely affected by progressive hydration (serpentinization) of the fore-arc mantle lithosphere (e.g. Schmidt and Poli 1998). This process controls the shape and internal circulation pattern of a subduction channel. Widening of the subduction channel due to hydration of the hanging wall mantle results in the onset of forced return flow in the channel. This may explain why the association of high- and/or ultrahigh-pressure metamorphic rocks with more or less hydrated (serpentinized) mantle material is often characteristic for high-pressure metamorphic complexes. Complicated non-steady geometry of weak hydrated subduction channels (Figs. 2.7, 2.9 and 2.11) was also predicted numerically (Gerya et al. 2006; Gorczyk et al. 2006, 2007a; Nikolaeva et al. 2008). This geometry forms in response to non-uniform water release from the slab that is controlled by metamorphic (dehydration) reactions in subducting rocks. Depleted mantle rocks from the base of the arc lithosphere and newly formed magmatic arc crust can be included into the channels (Figs. 2.11 and 2.12) at a mature stage of subduction (Nikolaeva et al. 2008).
- The shape of the P–T path, and the maximum P–T conditions achieved by an individual high-pressure metamorphic rock, depend on the specific trajectory of circulation in the subduction channel (Fig. 2.5). Both clockwise and counterclockwise

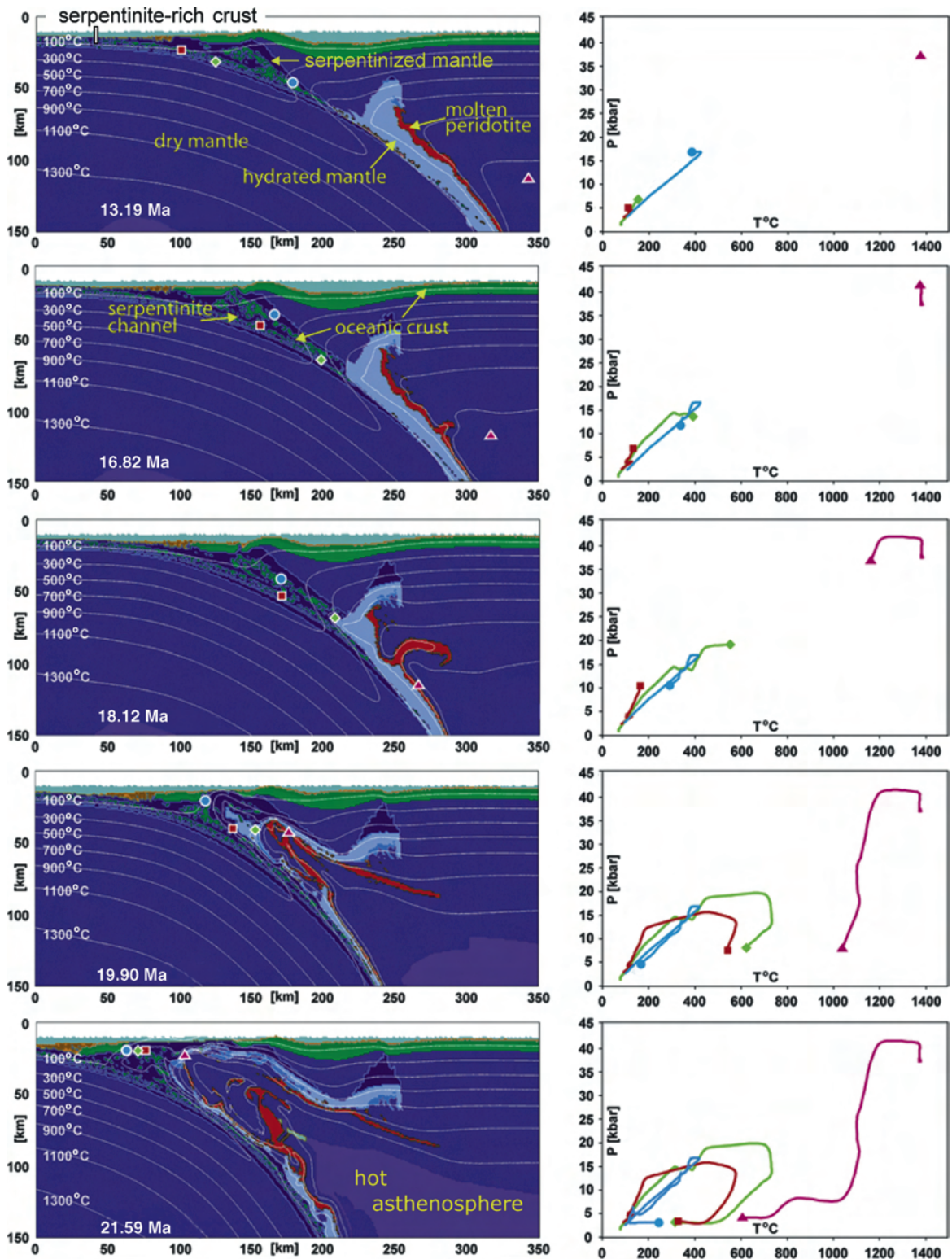


**Fig. 2.7** Exhumation of high- and ultrahigh-pressure rocks during retreating intra-oceanic subduction of an oceanic plate originated at slow spreading ridge (left columns) and character-

istic P-T paths of crustal and mantle rocks (right column). Results from 2D numerical modelling by Gorczyk et al. (2007a)

P–T paths are possible for fragments of oceanic crust that became involved in the circulation. Counterclockwise P–T paths are found for slices that are accreted to the hanging wall at an early stage of subduction, and set free by the progress of hydration and softening in a more evolved stage, returning towards the surface in a cooler environment. On the other hand, slices that were involved in continuous circulation, or that entered the subduction zone when a more stable thermal structure was already achieved, reveal exclusively clockwise trajectories. Model also indicates that P–T trajectories for the exhumation of high-pressure rocks in subduction channel fall into a P–T field of stability of antigorite in the mantle wedge (Fig. 2.6c).

- An array of diverse, though interrelated, P–T paths (Fig. 2.6c) rather than a single P–T trajectory is expected to be characteristic for subduction-related metamorphic complexes. The characteristic size and shape of the units with an individual history depend on the effective viscosity of the material in the subduction channel. Lower viscosities result in smaller characteristic length scales for coherent units and a marked contrasts between adjacent slices, a structure commonly termed melange, while higher viscosities favour the formation of extensive coherent nappes-like slices.

These conclusions based on relatively simple low-viscosity serpentinitized subduction channel model (Figs. 2.5 and 2.6a) were recently supported by petrological studies (e.g. Federico et al. 2007; Krebs et al. 2008) of subduction-related serpentinite mélanges. For example, Federico et al. (2007) tested the serpentinitized channel hypothesis by investigating a serpentinite mélange in the Western Alps, which contains exotic mafic and metasedimentary tectonic blocks, recording heterogeneous metamorphic evolutions and variable high-pressure ages. The peak metamorphic conditions range from eclogite- to garnet-blueschist-facies. The structural evidence and the pressure–temperature paths of the different blocks suggest coupling between blocks and matrix, at least in the blueschist facies.  $^{39}\text{Ar}$ – $^{40}\text{Ar}$  dating indicates eclogite-facies peak at ca. 43 Ma and blueschist-facies peak at ca. 43 and 40 Ma in different blocks, respectively. These data point to diachronous metamorphic paths resulting from independent tectonic evolutions of the different slices (compare with Figs. 2.5 and 2.6).

Krebs et al. (2008) presented coupled petrological and geochronological evidence from serpentinite melanges of the Rio San Juan Complex, Dominican Republic (Hispaniola) formed by intra-oceanic Caribbean subduction. It has been demonstrated that dispersed blocks of various types of metamorphic rocks in the mélanges provide fossil evidence for the dynamics of the subduction zone channel between 120 and 55 Ma. Based on three exemplary samples of eclogite and blueschist, a series of different but interrelated P–T–time paths was delineated. Eclogites indicate a low P/T gradient during subduction and record conditions in the nascent stages of the subduction zone with an anticlockwise P–T path (compare with Fig. 2.5, 6.4–15.3 Myr). Other blocks record the continuous cooling of the evolving subduction zone and show typical clockwise P–T-paths (compare with Fig. 2.5, 15.3–25.3 Myr). Omphacite blueschists correspond to the mature subduction zone recording very high (“cold”) P/T gradients. Cooling rates and exhumation rates of the metamorphic blocks were estimated to be 9–20°C/Ma and 5–6 mm/a, respectively. The derived P–T–time array is compared with the serpentinitized channel models (Gerya et al. 2002) with convergence rates of 10–40 mm/a resulting in an increasingly more funnel-shaped subduction channel system with time (Fig. 2.5). The numerically derived array of simulated P–T–time paths as well as the calculated rates of exhumation and cooling agree well with the P–T–time data derived from the metamorphic blocks of the Rio San Juan serpentinite mélanges when convergence rates of 15–25 mm/a are chosen (Krebs et al. 2008). This value is also in accord with available paleogeographic reconstructions calling for a long-term average of 22 mm/a of orthogonal convergence. On the basis of the comparison, the onset of subduction in the Rio San Juan segment of the Caribbean Great Arc can be constrained to approximately 120 Ma. This segment was thus obviously active for more than 65 Ma. An orthogonal convergence rate of 15–25 mm/a requires that a minimum amount of 975–1,625 km of oceanic crust must have been subducted. Both petrological/geochronological data and numerical simulation underscore the broad spectrum of different P–T–time paths and peak conditions recorded by material subducted at different periods of time as the subduction zone evolved and matured.

It has also been shown recently that not only high-pressure eclogites but also ultrahigh-pressure mantle

rocks (garnet-bearing peridotites) can be present in intra-oceanic subduction melanges (e.g. in Greater Antilles in Hispaniola, Abbott et al. 2006). Gorczyk et al. (2007a) modelled this phenomenon numerically (Fig. 2.7) and concluded that exhumation of such garnet-bearing peridotites can be related to fore-arc extension during subduction of an oceanic plate formed at a slow spreading ridge and characterized by serpentinite-rich crust. In this case subduction channel contains both serpentinites accreted from the subducting plate crust and progressively serpentinized fore-arc mantle. Intense rheological weakening of the mantle wedge takes place due to its strong hydration during subduction of water-rich crust formed at slow spreading ridge. This weakening triggers upwelling of the hydrated peridotites and partially molten peridotites followed by upwelling of hot asthenosphere and subsequent retreat of the subducting slab. According to numerical modelling of P–T paths this process can explain exhumation of UHP rocks in an intra-oceanic setting from depths of up to 120 km (4 GPa).

## 2.5 Magmatic Crust Growth and Thermal-Chemical Convection in the Mantle Wedge

Reymer and Schubert (1984) estimated rates of crustal generation during intra-oceanic subduction as 20–40 km<sup>3</sup>/km/Myr for the western Pacific region based on the total arc crust volume divided by the oldest known igneous age. More recent estimates for the same area by Taira et al. (Izu-Bonin island arc, 1998), Holbrook et al. (Aleutian island arc, 1999) and Dimalanta et al. (Tonga, New Hebrides, Marianas, Southern and Northern Izu-Bonin, Aleutian island arcs, 2002) are somewhat higher, 40–95 km<sup>3</sup>/km/Myr and are much higher, 120–180 km<sup>3</sup>/km/Myr, according to the work of Stern and Bloomer (early stage of IBM development, 1992). In particular, the arc magmatic addition rate of the arc of the New Hebrides varies between 87 and 95 km<sup>3</sup>/km/Myr as determined by Dimalanta et al. (2002). They also give values for addition rates of other island arcs, all of which vary between 30 and 70 km<sup>3</sup>/km/Myr. These values are average rates of crust production, calculated by dividing the estimated total volume of produced crust by the time in which it was produced and by the length of the arc.

It is commonly accepted that dehydration of subducting slabs and hydration of the overlying mantle wedges are key processes controlling magmatic activity and consequently crustal growth above subduction zones (e.g., Stern 2002; van Keken et al. 2002; van Keken and King 2005). Mantle wedge processes have been investigated from geophysical (e.g. Zhao et al. 2002; Tamura et al. 2002), numerical (e.g. Davies and Stevenson 1992; Iwamori 1998; Kelemen et al. 2004a; Arcay et al. 2005; Gerya et al. 2006; Nikolaeva et al. 2008), experimental (e.g., Poli and Schmidt 1995; Schmidt and Poli 1998), and geochemical (e.g., Ito and Stern 1986; Sajona et al. 2000; Kelley et al. 2006) perspectives. Indeed, detailed thermal structure and melt production patterns above slabs are still puzzling. Particularly, the relative importance of slab melting (e.g. Kelemen et al. 2004a; Nikolaeva et al. 2008) versus melting induced by simple thermal convection (Honda et al. 2002, 2007; Honda and Saito 2003) and/or thermal-chemical plumes (diapirs) (e.g. Tamura 1994; Hall and Kincaid 2001; Obata and Takazawa 2004; Gerya and Yuen 2003; Manea et al. 2005; Gerya et al. 2006; Gorczyk et al. 2007b; Zhu et al. 2009) to melt production in volcanic arcs is not fully understood.

Several authors (e.g., Tamura et al. 2002; Honda et al. 2007; Zhu et al. 2009) analyzed the spatial distribution of volcanism in Japan and concluded that several clusters of volcanism can be distinguished in space and time (Fig. 2.8). The typical spatial periodicity of such volcanic clusters is 50–100 km (see the spacing between “cigars” in Fig. 2.8b) while their life extent corresponds to 2–7 Myr (see the lengths of “cigars” in time in Fig. 2.8b). Two trench-parallel lines of volcanic density maxima can also be distinguished for some periods of intra-oceanic arc evolution (Fig. 2.8a). Spatial and temporal clustering of volcanic activity also associates with strongly variable (Fig. 2.4 in Calvert 2011) distribution of crustal thickness along intra-oceanic arcs (e.g. Figs. 2.4 and 2.5 in Calvert 2011; Kodaira et al. 2006, 2007) and distribution of seismic velocity anomalies in the mantle wedges under the arcs (e.g. Zhao et al. 1992, 2002; Zhao 2001; Tamura et al. 2002). This further points toward the relations between the mantle wedge processes and crustal growth in intra-oceanic arcs.

Based on 3D numerical models Honda and co-workers (Honda et al. 2002, 2007; Honda and Saito 2003; Honda and Yoshida 2005) proposed the

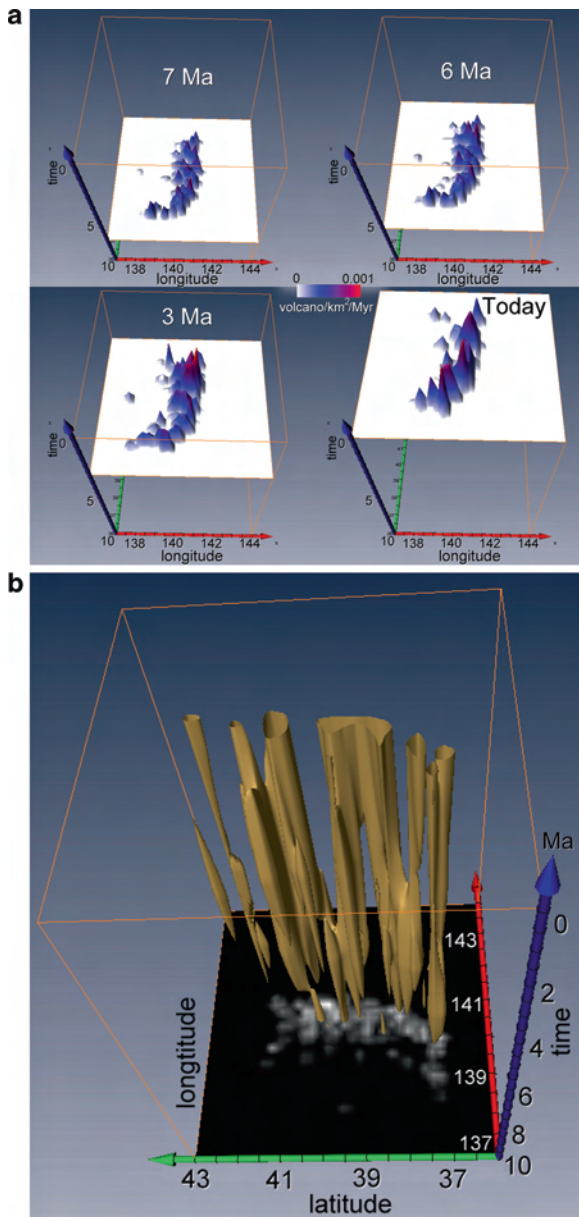


**Fig. 2.8** Variations in volcanic activity in NE Japan (Honda and Yoshida 2005; Honda et al. 2007; Zhu et al. 2009). (a) variations in the spatial density of volcanoes with their age during the past 10 Myr. (b) the isosurface of  $0.0003 \text{ volcano}/\text{km}^2/\text{Myr}$  for the observed density of volcanoes in space and time. The density of volcanoes notably evolves showing formation of spatially confined clusters that remain active within certain period of time that could be possibly related to the activity of mantle wedge plumes (cf. Fig. 2.10)

and Gurnis 2001; Conder and Wiens 2007; Honda and Saito 2003; Honda et al. 2002; Honda and Yoshida 2005; Arcay et al. 2005). These authors suggested that a roll (finger)-like pattern of hot (upwellings) and cold (downwellings) thermal anomalies emerges in the mantle wedge above the subducting slab contributing to clustering of magmatic activity at the arc surface. These purely thermal mantle wedge convection models, however, neglected chemical buoyancy effects coming from hydration and melting atop the subducting slab and leading to thermal-chemical convection and diapirism phenomena (e.g. Tamura 1994; Hall and Kincaid 2001; Gerya and Yuen 2003). These aspects have been recently studied numerically based on petrological-thermomechanical models including water transport and melting. These models predict

1. Spontaneous formation of a low viscosity wedge by hydration of the mantle atop the slab (Arcay et al. 2005; Zhu et al. 2009)
2. Growth of diapiric structures (“cold plumes”, Figs. 2.9 and 2.10) above the subducting slab (e.g., Gerya and Yuen 2003; Gorczyk et al. 2007b; Zhu et al. 2009)
3. Broad variation in seismic velocity beneath intraoceanic arcs due to hydration and melting (Gerya et al. 2006; Nakajima and Hasegawa 2003a, b; Gorczyk et al. 2006; Nikolaeva et al. 2008)
4. Variations in melt production and crustal growth processes caused by propagation of hydrated plumes in the mantle wedge (Gorczyk et al. 2007b; Nikolaeva et al. 2008; Zhu et al. 2009)

Nikolaeva et al. (2008) investigated crustal growth processes on the basis of a 2D coupled petrological-thermomechanical numerical model of retreating intraoceanic subduction (Figs. 2.11 and 2.12). The model included spontaneous slab retreat and bending, subducted crust dehydration, aqueous fluid transport, mantle wedge melting, and melt extraction resulting in crustal growth. As follows from the numerical experiments the rate of crust formation is strongly variable with time and positively correlates with subduction rate (Fig. 2.11, bottom diagram). Modelled average rates of crustal growth ( $30\text{--}50 \text{ km}^3/\text{km}/\text{Ma}$ , without effects of dry decompression melting) are close to the lower edge of the observed range of rates for real intraoceanic arcs ( $40\text{--}180 \text{ km}^3/\text{km}/\text{Ma}$ ). The composition of new crust depends strongly on the evolution of subduction. Four major magmatic sources can contribute

697 development of small-scale thermally driven convec-  
 698 tion in the uppermost corner of the mantle wedge with  
 699 lowered viscosity (low viscosity wedge, LVW, Billen

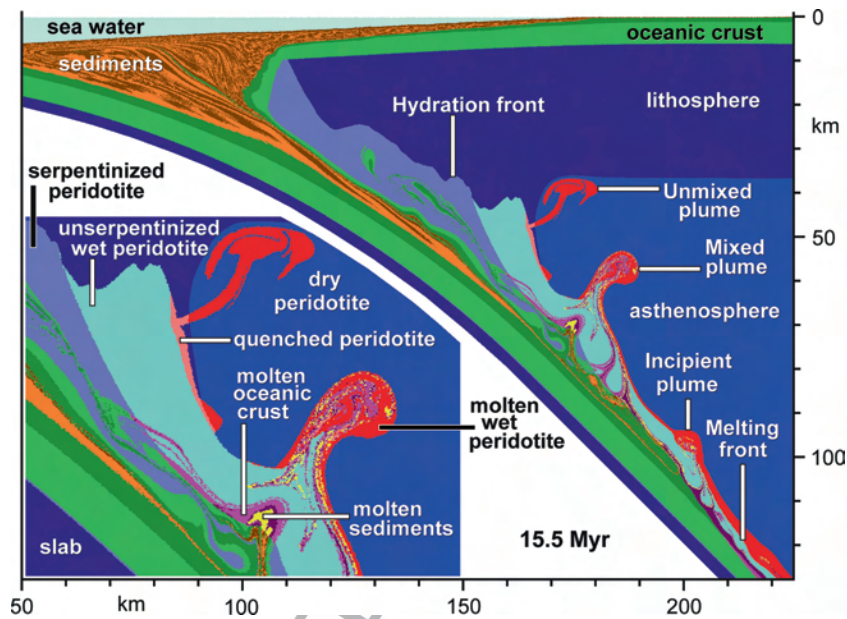


**Fig. 2.9** Development of unmixed and mixed plumes due to hydration of the mantle wedge by fluids released from the slab. Plumes rising from the slab are colder than the surrounding mantle wedge (see Fig. 2.10a for 3D thermal structures around such plumes). The corrugations along the hydration front reflect

dynamics of slab dehydration controlled by metamorphic reactions. Zoomed area shows lithological structures of mixed and unmixed plumes. Results from 2D numerical modelling by Gerya et al. (2006)

748 to the formation of the crust: (1) hydrated partially  
749 molten peridotite of the mantle wedge, (2) melted  
750 subducted sediments, (3) melted subducted basalts,  
751 (4) melted subducted gabbro. Crust produced from  
752 the first source is always predominant and typically  
753 comprise more than 95% of the growing arc crust  
754 (Nikolaeva et al. 2008). In all studied cases, it appears  
755 shortly after beginning of subduction and is a persis-  
756 tent component so long as subduction remains active.  
757 Significant amount of crust produced from other three  
758 sources appear (1) in the beginning of subduction due  
759 to the melting of the slab “nose” and (2) at later stages  
760 when subduction velocity is low (<1 cm/a), which  
761 leads to the thermal relaxation of the slab. Both the  
762 intensity of melt extraction, and the age of subducted  
763 plate affect the volume of new crust. On a long time  
764 scale the greatest volume of magmatic arc crust is  
765 formed with an intermediate melt extraction threshold  
766 (2–6%) and medium subducted plate ages (70–100 Ma)  
767 (Nikolaeva et al. 2008).

768 Recently thermal-chemical mantle wedge convec-  
769 tion and related melt production dynamics (Fig. 2.10)  
770 were also examined numerically in 3D (Zhu et al.  
771 2009; Honda et al. 2010). Honda et al. (2010) analysed

772 simple subduction model including moderately buoy- 772  
773 ant chemical agent (water) and found that the hydrated 773  
774 region tends to stay in the corner of the mantle wedge 774  
775 because of its low density and this results in the low 775  
776 temperature zone (“cold nose”) there. Moderate chemi- 776  
777 cal buoyancy present in the mantle wedge may either 777  
778 suppress or shift toward the back arc the thermally 778  
779 driven small-scale convection under the arc and 779  
780 make the dominant mantle flow velocity to be normal 780  
781 to the plate boundary. Zhu et al. (2009) examined 781  
782 more complex 3-D petrological-thermomechanical 782  
783 model of intra-oceanic subduction focussing on geo- 783  
784 metries and patterns of hydrous thermal-chemical 784  
785 upwellings (“cold plumes”) formed above the slab 785  
786 (Figs. 2.9 and 2.10). These numerical simulations 786  
787 showed that three types of plumes occur above the 787  
788 slab: (a) finger-like plumes that form sheet-like struc- 788  
789 ture parallel to the trench (Fig. 2.10a, b); (b) ridge-like 789  
790 structures perpendicular to the trench; (c) flattened 790  
791 wave-like instabilities propagating upwards along the 791  
792 upper surface of the slab and forming zig-zag patterns 792  
793 subparallel to the trench. 793

794 Zhu et al. (2009) also computed spatial and tempo- 794  
795 ral pattern of melt generation (i.e. crust production) 795

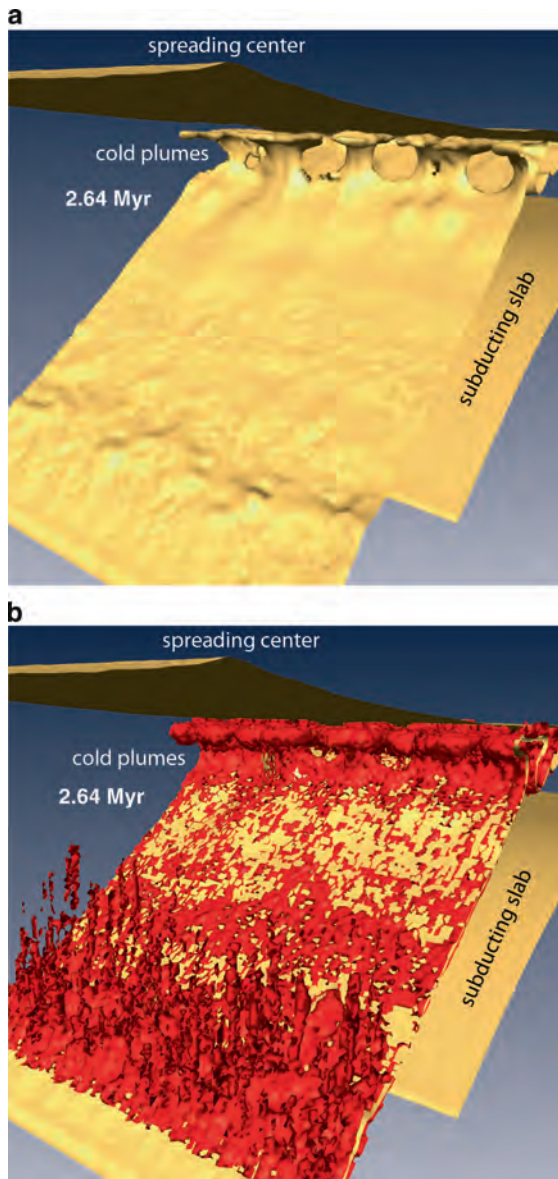
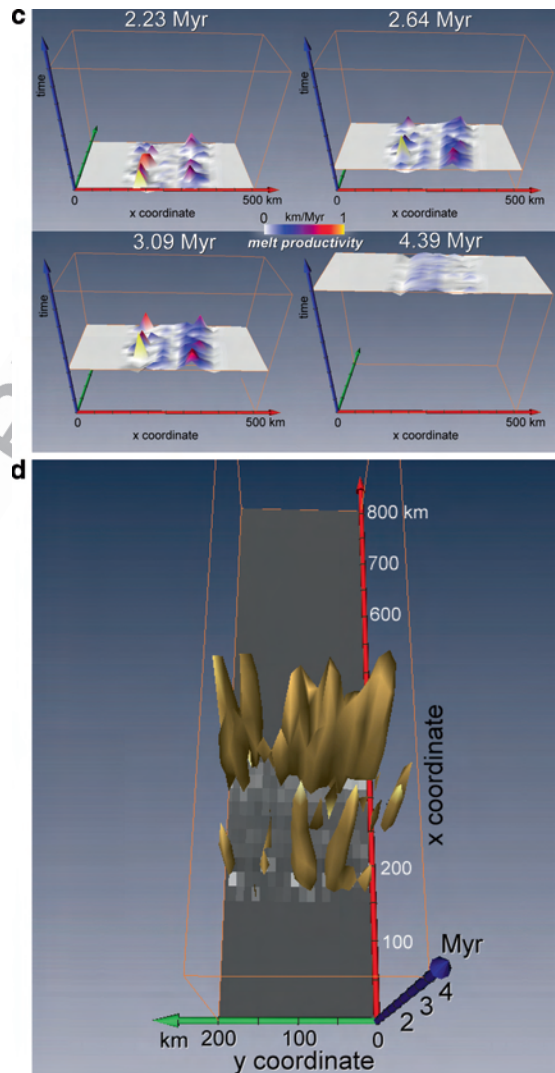


Fig. 2.10 (continued)



**Fig. 2.10** Thermal-chemical plumes (a, b) growing in the mantle wedge during intra-oceanic subduction and corresponding variations of melt production (c, d). (a) the 1,350 K isosurface of temperature at 2.64 Myr, note that plumes rising from the slab are colder than the surrounding mantle wedge. (b) same temperature isosurface (yellow) with partially molten rocks, which are responsible for plume buoyancy, shown in red. (c) variations in the spatial intensity of melt production beneath the surface, peaks in the melt production correspond to individual thermal-chemical plumes shown in (a). (d) the isosurface of  $0.6 \text{ km}^3/\text{km}^2/\text{Myr}$  for melt production, which implies crustal growth intensity of 600 m/Myr. Results from 3D numerical modelling by Zhu et al. (2009)

796 intensity above the slab, which appeared to be strongly  
 797 controlled by the hydrous plume activities (Fig. 2.10c,  
 798 d). Peaks of the melt production projected to the arc  
 799 surface at different moments of time (Fig. 2.10c)  
 800 always indicate individual thermal-chemical plumes  
 801 growing at that time. Such peaks often form the linear  
 802 structure close to the trench, and another line of peaks  
 803 in linear pattern, which is approximate 200 km away  
 804 from the trench. The former ones are mainly from the  
 805 depth of 50–70 km; the latter ones are mainly from

the depth of 140–170 km. Figure 2.10d shows the  
 806 melt productivity in time by visualizing the isosur-  
 807 face ( $0.6 \text{ km}^3/\text{km}^2/\text{Myr}$ ) of melt production intensity.  
 808 The plume-like structures are reflected by distinct  
 809

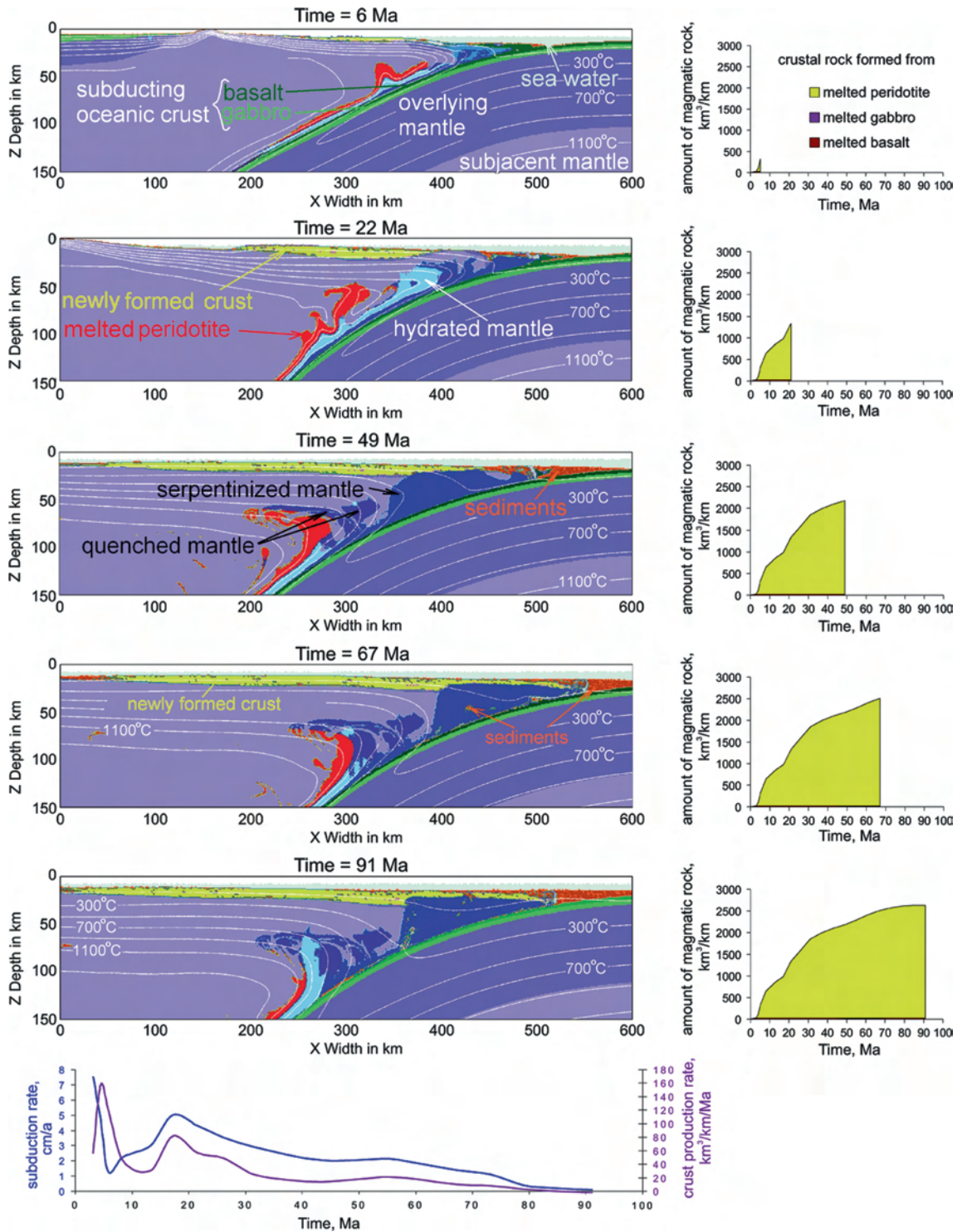


**Fig. 2.11** Dynamics of a pure retreating intra-oceanic subduction (left column) and associated magmatic crust growth (right column). Spontaneous changes in subduction rate (for this model subduction rate and trench retreat rate are equal) and crust accumulation rate with time are depicted below. Time is

dated from the beginning of subduction. Subduction results in a hydration and partial melting of mantle wedge rocks, which leads to the formation of volcanic arc rocks (yellow) above the area of melting. Results from 2D numerical modelling by Nikolaeva et al. (2008)

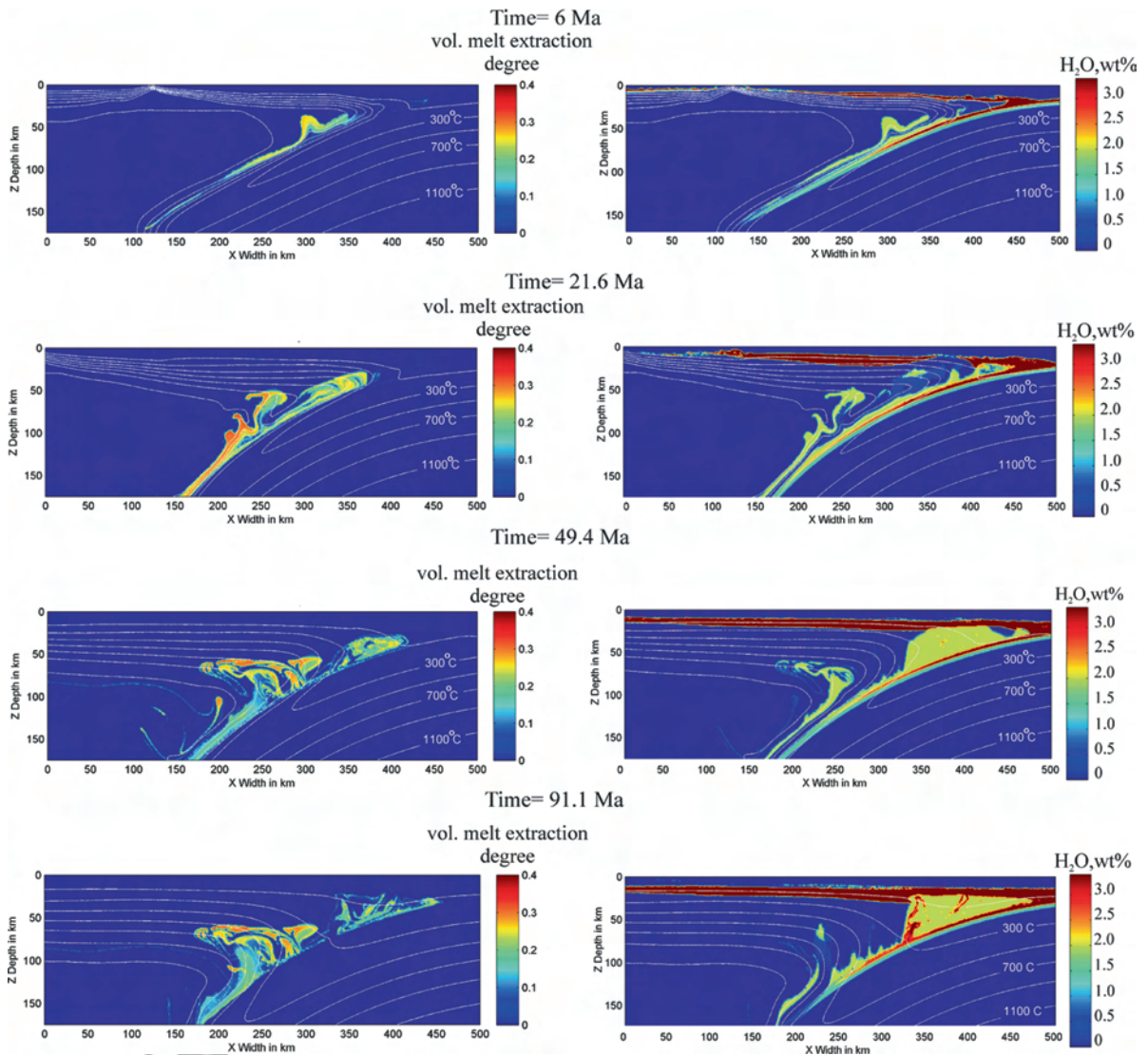


**Fig. 2.12** Evolution of degree of melt extraction (left column) and water content (right column) in the mantle wedge and subducting oceanic crust. Corresponding lithological field is

depicted on the Fig. 2.11. Results from 2D numerical modelling by Nikolaeva et al. (2008)

810 “cigar-like” features that are bounded in both time and  
 811 space (Fig. 2.10d). Each “cigar” corresponds to the  
 812 activity of a distinct plume that (1) increases the melt  
 813 productivity during the early stage when the growing  
 814 melt production is related to decompressing and heating  
 815 of the rising plume material and (2) decreases the  
 816 melt productivity during the later stage when the temperature,  
 817 the pressure and the degree of melting stabilize inside the  
 818 horizontally spreading and thermally relaxing plume.  
 819

The modelled wavelength (25–100 km) and the  
 growth time (2–7 Myr, see the lengths of “cigars” in  
 time in Fig. 2.10d) of the thermal-chemical plumes are  
 comparable to spatial periodicity (50–100 km) and the  
 life extent (2–7 Myr, see the lengths of “cigars” in time  
 in Fig. 2.8b) of volcanic clusters and to spatial periodicity  
 (50–100 km, Fig. 2.4b in Calvert 2011) of crustal  
 thickness variations in intra-oceanic arcs. The existence  
 of two contemporaneous trench-parallel lines  
 of melt productivity (Fig. 2.10b) is also similar to the

830 natural observations (see two trench-parallel lines of  
831 Quaternary volcanic density maxima in Fig. 2.8a, at  
832 6 Ma). To explain such phenomena, Wyss et al. (2001)  
833 have proposed an additional source of fluids to be  
834 located at the top of the slab (at about 150 km depth).  
835 Their proposition is based on the velocity tomography  
836 in the mantle wedge above the slab, and on the map-  
837 ping of earthquake size distribution within the mantle  
838 wedge. Geochemical evidence (Kimura and Yoshida  
839 2006) for Quaternary lavas from the NE Japan arc also  
840 shows the deeper mantle-derived rear-arc lava coming  
841 from 100–150 km depth.

## 842 2.6 Geochemistry of Intra-oceanic Arcs

843 The role of subduction zones in global geochemical  
844 dynamics is generally twofold: first, crustal materials  
845 are recycled back into the deep mantle, and second,  
846 new crust is produced in magmatic arcs above subduc-  
847 tion zones (e.g. Bourdon et al. 2003). Because the  
848 physical and chemical changes within the subducting  
849 plate and mantle wedge are largely inaccessible to a  
850 direct observation, geochemical investigations con-  
851 centrate on the input (rocks subducted atop the slabs)  
852 and output (magmatic products of island arcs) signals  
853 of subduction zones (e.g., Plank and Langmuir 1993;  
854 Hauff et al. 2003). For example, as discussed by  
855 Kimura and Yoshida (2006), Quaternary lavas from  
856 NE Japan arc show geochemical evidence of mixing  
857 between mantle-derived basalts and crustal melts at  
858 the magmatic front, whereas significant crustal signals  
859 are not detected in the rear-arc lavas.

860 Analyses of comprehensive geochemical data sets  
861 for the input and output rock-members (Hauff et al.  
862 2003) from several arc systems such as Aleutian  
863 (Yogodzinski, 2001), Izu-Bonin-Mariana (Tatsumi  
864 et al. 2008), New Britain, Vanuatu (Arai and Ishimaru  
865 2008), Kamchatka (Churikova et al. 2001; Dosseto  
866 et al. 2003; Yogodzinski et al. 2001) and Tonga-  
867 Kermadec arcs (Turner and Hawkesworth 1997) lead  
868 to the conclusion that subduction-related arc basalts  
869 (output signal) characteristically have elevated con-  
870 tents of large-ion lithophile element (LILEs) and  
871 light rare earth element (LREEs) with depleted  
872 heavy REE (HREE) and high field strength elements  
873 (HFSEs) compared to subducted crust (input signal)  
874 (McCulloch and Gamble 1991; Elliott et al. 1997;

Elliott 2003; Plank and Langmuir 1993; Kimura 875  
et al. 2009). In relation to that, the following processes 876  
are believed to be responsible for the element parti- 877  
tioning in intra-oceanic arc magmas (e.g. Kimura et al. 878  
2009 and reference therein): 879

- Extraction of fluids and/or melts from the sub- 880  
ducted slab; combined slab fluid and melt fluxes 881  
may be responsible for geochemical variations 882  
along or across magmatic arcs (Eiler et al. 2005; 883  
Ishizuka et al. 2006); separate deep and shallow 884  
slab components have also been proposed (Kimura 885  
and Yoshida 2006; Pearce and Peate 1995; Pearce 886  
et al. 2005) 887
- Fluid fluxed melting of the mantle wedge responsi- 888  
ble for generation of high-MgO primitive arc 889  
basalts (Arculus and Johnson 1981; Davidson 890  
1996; Elliott et al. 1997; Hawkesworth et al. 891  
1993; Kelemen et al. 1998; Kimura and Yoshida 892  
2006; Plank and Langmuir 1993; Poli and Schmidt 893  
1995; Stern 2002; Stolper and Newman 1994; 894  
Tatsumi and Eggins 1995; Turner et al. 1997) 895
- Slab melt–mantle reaction generating high-MgO 896  
primitive arc andesites (Kelemen et al. 2004b; 897  
Tatsumi and Hanyu 2003; Tsuchiya et al. 2005; 898  
Yogodzinski et al. 1994; Zack et al. 2002) 899
- Melting of mantle wedge metasomatized by slab- 900  
derived fluid or melt (Eiler et al. 2007; Sajona et al. 901  
1996) 902
- Direct supply of felsic melt from eclogitic slab 903  
melting (Defant and Drummond 1990; Martin 904  
1999; Martin et al. 2005) 905
- Melting of hydrated mantle and subducted tectonic 906  
melanges in respectively unmixed and mixed ther- 907  
mal-chemical plumes (Fig. 2.9) rising from the top 908  
of the slab (Tamura 1994; Gerya et al. 2006; Castro 909  
and Gerya 2008; Castro et al. 2010) 910

Despite the broad variability of involved geochem- 911  
ical mechanisms currently there is a consensus (e.g. 912  
Kimura et al. 2009) about the relative significance of 913  
various processes and it is widely believed that slab 914  
dehydration or melting combined with the interaction 915  
of this slab-derived flux with variously depleted man- 916  
tle generates primary arc magmas with the observed 917  
geochemical characteristics. These primary magmas 918  
typically have radiogenic Sr and Pb isotopic composi- 919  
tion, with less radiogenic Nd in lavas erupted from the 920  
volcanic front compared to rear-arc magmas appar- 921  
ently derived from more depleted upper mantle 922

AU5

AU6

923 sources (Elliott et al. 1997; Ishizuka et al. 2003;  
 924 Kelemen et al. 2004b; Kimura and Yoshida 2006;  
 925 Manning 2004; Rapp and Watson 1995; Stolper and  
 926 Newman 1994; Tatsumi and Eggins 1995).

927 Elliott (2003) and other authors (Hawkesworth  
 928 et al. 1993; Leat and Larter 2003; McCulloch and  
 929 Gamble 1991; Stern 2002) describe two distinct  
 930 major slab components present in arc rocks with dif-  
 931 ferent sources and transport mechanisms: (1) melt of  
 932 the down-going sediments, and (2) aqueous fluid  
 933 derived from altered oceanic crust. Direct melting of  
 934 the slab is also suggested as a possible mechanism for  
 935 melts generation (e.g. Defant and Drummond 1990;  
 936 Martin 1999; Martin et al. 2005; Kelemen et al. 2004a;  
 937 Nikolaeva et al. 2008). Fluids and melts liberated from  
 938 subducting oceanic crust produce melting above slabs  
 939 and finally lead to efficient subduction-zone arc volca-  
 940 nism (Fig. 2.4). The exact composition of the mobile  
 941 phases generated in the subducting slab have however,  
 942 remained incompletely known (e.g. Kessel et al.  
 943 2005). In this respect the fundamental control appears  
 944 to be (e.g. Kimura et al. 2009) the P–T paths of rocks  
 945 in the subducting slab, which can be approximated by  
 946 geodynamic modelling (e.g., Peacock and Wang 1999;  
 947 Gerya and Yuen 2003; Castro and Gerya 2008). For  
 948 example in the model of Peacock and Wang (1999),  
 949 subduction of old and cold oceanic plate leads to low  
 950 slab surface temperature. In contrast, subduction of  
 951 young and hot oceanic crust typically results in higher  
 952 slab surface temperatures (Stern et al. 2003).

953 Such contrasting thermomechanical behaviour can  
 954 presumably be observed in the arcs of Japan (Peacock  
 955 and Wang 1999), where the old Pacific Plate (>120 Ma,  
 956 NE Japan) and the young Shikoku Basin (15–27 Ma,  
 957 SW Japan) are subducting beneath the Eurasia plate  
 958 (Kimura and Stern 2009; Kimura et al. 2005; Kimura  
 959 and Yoshida 2006). Consequently, in NE Japan slab  
 960 dehydration seems to dominate geochemical signal in  
 961 the primary arc basalts (Kimura and Yoshida 2006;  
 962 Moriguti et al. 2004; Shibata and Nakamura 1997),  
 963 whereas in SW Japan slab melting is proposed to be  
 964 responsible for generation of high-MgO andesites or  
 965 adakitic dacites (Kimura and Stern 2009; Kimura et al.  
 966 2005; Shimoda and Nohda 1995; Tatsumi and Hanyu  
 967 2003). Recently Kimura et al. (2009) obtained similar  
 968 results from simulations of geochemical variability of  
 969 primitive magmas across an intra-oceanic arc based on  
 970 partitioning of incompatible element and Sr-Nd-Pb  
 971 isotopic composition in a slab-derived fluid and in

arc basalt magma generated by an open system fluid- 972  
 fluxed melting of mantle wedge peridotite (Fig. 2.4). 973  
 Similar contrasting geochemical behaviour has been 974  
 also shown (e.g. Kimura et al. 2009 and reference 975  
 therein) between arcs along the western and eastern 976  
 Pacific rims. Arc magmatism due to slab-derived 977  
 fluids is proposed for the western Pacific arcs, includ- 978  
 ing the Kurile, NE Japan, and the Izu-Bonin-Mariana 979  
 arcs (Ishikawa and Nakamura 1994; Ishikawa and 980  
 Tera 1999; Ishizuka et al. 2003; Kimura and Yoshida 981  
 2006; Moriguti et al. 2004; Pearce et al. 2005; Ryan 982  
 et al. 1995; Straub and Layne 2003). High-MgO 983  
 primary mafic magmas from these relatively cold 984  
 subduction zones show geochemical signatures of 985  
 extremely fluid mobile elements such as B, Li, or U 986  
 (Ishikawa and Nakamura 1994; Ishikawa and Tera 987  
 1999; Moriguti et al. 2004; Ryan et al. 1995; Turner 988  
 and Foden 2001). In contrast, slab melting better 989  
 explains the origin of high-MgO intermediate lavas 990  
 in the eastern Pacific (Kelemen et al. 2004b; Straub 991  
 et al. 2008) although the role of slab fluid remains an 992  
 important factor in some of the arcs (Grove et al. 993  
 2006). 994

Alternative ideas that explain broad variability of 995  
 slab fluid and slab melt geochemical components in 996  
 arc magmas were proposed recently based on petrolo- 997  
 gical-thermomechanical numerical modeling of sub- 998  
 duction zones (Gerya et al. 2006; Castro and Gerya 999  
 2008; Castro et al. 2010). Gerya et al. (2006) sug- 1000  
 gested that one possibility for transporting two distinct 1001  
 geochemical signatures through the mantle wedge can 1002  
 be related to generation and propagation of partially 1003  
 molten compositionally buoyant diapiric structures 1004  
 (cold plumes, Tamura 1994; Hall and Kincaid 2001; 1005  
 Gerya and Yuen 2003) forming atop the slab. Numerical 1006  
 experiments of Gerya et al. (2006) show that two 1007  
 distinct types of plumes can form in the mantle wedge 1008  
 (Fig. 2.9): 1009

1. Mixed plumes form atop the slab and consist of 1010  
 partially molten mantle and recycled sediments 1011  
 mixed on length-scales of 1–100 m (i.e. subducted 1012  
 tectonic melange). Magma production from such 1013  
 compositionally heterogeneous plumes may pro- 1014  
 duce a strong crustal melt signature in resulting 1015  
 magmas. 1016
2. Unmixed plumes form above the slab and consist 1017  
 of hydrated partially molten mantle located at 1018  
 a distance from the slab, which is therefore not 1019

1020 mechanically mixed with subducted crustal rocks.  
1021 Magma production from such hydrated but compo-  
1022 sitionally homogeneous plumes may produce a  
1023 pronounced slab fluid signature.

1024 These distinct plume types can explain the presence  
1025 of different magmas in volcanic arcs (e.g., Stern  
1026 2002): magmas with distinct crustal signatures (e.g.,  
1027 adakites) and primitive magmas from peridotitic  
1028 source (e.g., arc tholeiites). Thermal zoning inside  
1029 rapidly rising unmixed cold plumes can result in tran-  
1030 sient bimodal magmatism because of both the compo-  
1031 sitional and the thermal zoning of these structures  
1032 (Fig. 2.10a, b), which would generate basalts from  
1033 its water-depleted, hot rinds, and boninites from  
1034 its water-enriched, cooler interiors (Tamura 1994).  
1035 Rates of plume propagation vary between several cen-  
1036 timeters to meters per year (Gerya and Yuen 2003;  
1037 Gerya et al. 2004) corresponding to 0.1–3 Myr transfer  
1038 time through the asthenospheric portion of the mantle  
1039 wedge. This is consistent with U–Th isotope measure-  
1040 ments from island arc magmas that suggest short  
1041 transfer times for fluids (0.03–0.12 Myr) and slab-  
1042 derived melts (several Myr) (Hawkesworth et al.  
1043 1997). It is noteworthy that the diapiric transport  
1044 (e.g. Tamura 1994; Hall and Kincaid 2001) of various  
1045 geochemical components in the mantle wedge does  
1046 not require melting of subducted crust immediately  
1047 at the slab surface (e.g. Kelemen et al. 2004a). Intense  
1048 melting of subducted sediments and oceanic crust in  
1049 the mixed plumes occurs in the temperature range of  
1050 900–1,400°C (Gerya and Yuen 2003; Gerya et al.  
1051 2006; Castro and Gerya 2008; Castro et al. 2010)  
1052 after penetration of these structures into the hot portion  
1053 of the mantle wedge. This behaviour agrees well with  
1054 geochemical models suggesting notable sediment  
1055 melting beneath the arc, behaviour which is otherwise  
1056 not trivial to reconcile (e.g. Kelemen et al. 2004a) with  
1057 low slab surface temperature inferred from thermal  
1058 models for subduction zones as discussed by George  
1059 et al. (2003).

1060 Mixed cold plumes composed of tectonic melanges  
1061 derived from subduction channels can transport the  
1062 fertile subducted crustal materials towards hotter  
1063 zones of the suprasubduction mantle wedge leading  
1064 to the formation of silicic melts. Recently magmatic  
1065 consequences of this plausible geodynamic scenario  
1066 were evaluated by using an experimental approach  
1067 (Castro and Gerya 2008; Castro et al. 2009, 2010).

Melt compositions, fertility and reaction between  
silicic melts and the peridotite mantle (both hydrous  
and dry) were tested by means of piston–cylinder  
experiments at conditions of 1,000°C and pressures  
of 2.0 and 2.5GPa. The results indicate that silicic  
melts of trondhjemite and granodiorite compositions  
may be produced in the ascending mixed plume mega-  
structures. Experiments show that the formation of an  
Opx-rich reaction band, developed at the contact  
between the silicic melts and the peridotite, protect  
silicic melts from further reaction in contrast to the  
classical view that silicic melts are completely con-  
sumed in the mantle. It has also been demonstrated  
experimentally (Castro et al. 2010) that the compo-  
sition of melts formed after partial melting of sediment-  
MORB mélanges is buffered for broad range of  
sediment-to-MORB ratios (from 3:1 to 1:3), producing  
liquids along a cotectic of granodiorite to tonalite  
composition in lower-variance phase assemblage  
Melt+Grt+Cpx+Pl. The laboratory experiments, there-  
fore, predict decoupling between major element and  
isotopic compositions: large variations in isotopic  
ratios can be inherited from a compositionally hetero-  
geneous source but major element compositions can  
be dependent on the temperature of melting rather than  
on the composition of the source (Castro et al. 2010).

Important geochemical constrains concerns distri-  
bution and amount of water above subduction zones  
that impose strong controls on chemistry of magmatic  
arc rocks forming at the surface (e.g., Kelley et al.  
2006 and references therein). Flux of water originating  
from the dehydrating, subducting slab lowers the man-  
tle solidus (e.g., Kushiro et al. 1968) triggering melt-  
ing of the mantle wedge beneath arcs and back-arc  
basins (Fig. 2.4). This is supported by a range of  
various widespread observations on subduction zone  
lavas (e.g., Kelley et al. 2006 and references therein),  
seismological data (e.g. Tamura et al. 2002; Jung  
and Karato 2001; Iwamori 2007) and numerical mod-  
elling constrains (Iwamori 1998; Arcay et al. 2005;  
Nikolaeva et al. 2008; Hebert et al. 2009).

Back-arc basins related to intra-oceanic subduction  
(Fig. 2.4) are natural places to investigate water-related  
processes in the mantle wedge because these settings  
can be treated, in many ways, like mid-ocean ridges  
(Kelley et al. 2006). Particularly, the driest back-arc  
basin melts (Fig. 2.13) are compositionally equivalent  
to mid-ocean ridge melts and can be interpreted  
as melts generated by decompression melting of

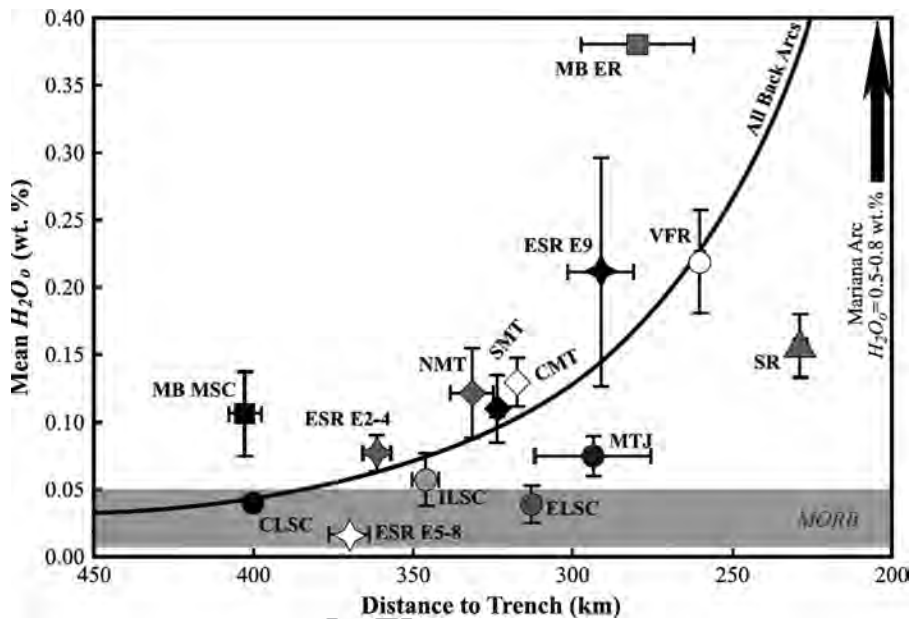


**Fig. 2.13** Mean water content in the mantle source ( $H_2O$ ) versus distance to the trench at back-arc basins (Kelley et al. 2006). The back-arc basin data are regional averages of the Manus basin Eastern Rifts (MB ER) and the Manus spreading center/eastern transform zone (MB MSC), the Lau basin central Lau spreading center (CLSC), the intermediate Lau spreading center (ILSC), the Mangatolu triple junction (MTJ), the eastern

Lau spreading center (ELSC) and the Valu Fa ridge (VFR), the East Scotia ridge segments (ESR E2–E4, ESR E5–E8, ESR E9), and the Mariana trough northern third (NMT), central third (CMT) and southern third (SMT). The shaded field is the range of  $H_2O$  in MORB from the same study. The black arrow indicates the direction that volcanic arcs are predicted to plot (Kelley et al. 2006)

1117 ascending mantle (Fig. 2.4). Geochemical studies of  
 1118 back arcs related to intra-oceanic subduction (e.g.  
 1119 Stolper, and Newman 1994; Taylor and Martinez  
 1120 2003; Kelley et al. 2006) demonstrated the hybrid  
 1121 nature of the back-arc basin melting process:  
 1122 MORB-like geochemistry found in relatively dry  
 1123 back-arc melts is systematically perturbed in wetter  
 1124 samples affected by the addition of  $H_2O$ -rich material  
 1125 from the subducted slab (Fig. 2.13).

1126 Recently Kelley et al. (2006) examined data com-  
 1127 piled from six back-arc basins and three mid-ocean  
 1128 ridge regions and evaluated concentration of  $H_2O$  in  
 1129 the mantle source based on measured  $H_2O$  concentra-  
 1130 tions of submarine basalts collected at different dis-  
 1131 tances from the trench (Fig. 2.13). This study clearly  
 1132 demonstrated that water concentrations in back-arc  
 1133 mantle sources increase toward the trench, and back-  
 1134 arc spreading segments with the highest water content  
 1135 are at anomalously shallow water depths, consistent  
 1136 with increases in crustal thickness and total melt  
 1137 production resulting from high  $H_2O$ . In contrast  
 1138 to mid ocean ridges, back-arc basin spreading com-  
 1139 bines ridge-like adiabatic decompression melting with

nonadiabatic mantle melting paths that may be inde- 1140  
 pendent of the solid flow field and depend on the  $H_2O$  1141  
 supply from the subducting plate (Kelley et al. 2006). 1142  
 This conclusion is also consistent with numerical 1143  
 modelling results (e.g. Iwamori 1998; Arcay et al. 1144  
 2005; Nikolaeva et al. 2008; Honda et al. 2010) pre- 1145  
 dicting that water-rich mantle sources should mainly 1146  
 concentrate at 100–250 km distances from the trench 1147  
 in proximity of water-rich, depleted and chemically 1148  
 buoyant “cold nose” of the mantle wedge (Figs. 2.11 1149  
 and 2.12). 1150

## 2.7 Conclusions 1151

The following messages are “to take home” from this 1152  
 chapter: 1153

- Modern intra-oceanic subduction zones comprise 1154  
 around 40%, of the convergent margins of the 1155  
 Earth and most of them are not accreting sediments 1156  
 and have back-arc extension. 1157

- 1158 • It is not yet entirely clear where and how intra-  
 1159 oceanic subduction initiates although two major  
 1160 types of subduction zone nucleation scenarios are  
 1161 proposed: induced and spontaneous.
- 1162 • Internal structure and compositions of intra-oceanic  
 1163 arcs is strongly variable. Both along- and across-arc  
 1164 variation of crustal thickness and lithological struc-  
 1165 ture are inferred based on seismological data and  
 1166 numerical modeling.
- 1167 • Base of the arc includes crust–mantle transitional  
 1168 layer of partly enigmatic origin (cumulates?, repla-  
 1169 cative rocks?, intercalation of various rocks and  
 1170 melts?) and imprecisely known thickness.
- 1171 • Major element composition of magmas feeding  
 1172 arcs from the mantle is debatable, particularly  
 1173 regarding the MgO content of erupted basaltic  
 1174 magmas which are too MgO-poor to represent  
 1175 the parental high-MgO mantle-derived magma.  
 1176 Magma fractionation and reactive flow models are  
 1177 suggested to explain this MgO-paradox.
- 1178 • Exhumation of high- and ultrahigh-pressure crustal  
 1179 and mantle rocks during intra-oceanic subduction  
 1180 are strongly controlled by serpentized subduction  
 1181 channels forming by hydration of the overriding  
 1182 plate and incorporation of subducted upper oceanic  
 1183 crust. Newly formed volcanic rocks and depleted  
 1184 mantle from the base of the arc lithosphere can be  
 1185 included into subduction channels at a mature stage  
 1186 of subduction.
- 1187 • An array of diverse both clockwise and counter  
 1188 clockwise P–T–time paths rather than a single P–T  
 1189 trajectory is characteristic for high-pressure rock  
 1190 melanges forming in the serpentized channels.
- 1191 • Crustal growth intensity in intra-oceanic arcs  
 1192 (40–180 km<sup>3</sup>/km/Myr) is variable in both space  
 1193 and time and should strongly depend on subduction  
 1194 rate as well as on intensity and character of  
 1195 thermal-chemical convection in the mantle wedge  
 1196 driven by slab dehydration and mantle melting.  
 1197 This convection can possibly include hydrated  
 1198 diapiric structures (cold plumes) rising from the  
 1199 slab and producing silicic magmatic rocks by melt-  
 1200 ing of subducted rock melanges.
- 1201 • Subduction-related arc basalts (output signal) char-  
 1202 acteristically have elevated contents of large-ion  
 1203 lithophile element (LILEs) and light rare earth ele-  
 1204 ment (LREEs) with depleted heavy REE (HREE)  
 1205 and high field strength elements (HFSEs) compared  
 1206 to subducted oceanic crust (input signal).
- The exact origin of geochemical variations in arc  
 basalts is debatable and may involve a range of  
 processes such as (a) extraction of fluids and/or  
 melts from the subducted slab, (b) fluid fluxed and  
 decompression melting of the mantle wedge, (c)  
 slab melt–mantle reactions, (d) melting of mantle  
 wedge metasomatized by slab-derived fluid or melt,  
 (e) direct supply of felsic melt from eclogitic slab  
 melting, (f) melting of hydrated mantle and sub-  
 ducted tectonic melanges in thermal-chemical  
 plumes.
- Water concentrations in back-arc mantle sources  
 increase toward the trench. Back-arc basin spread-  
 ing combines mid-ocean-ridge-like adiabatic  
 decompression melting with nonadiabatic fluid-  
 fluxed mantle melting depending on the H<sub>2</sub>O sup-  
 ply from the subducting plate. Numerical modeling  
 results predict that water-rich mantle sources  
 should mainly concentrate at 100–250 km distances  
 from the trench in proximity of water-rich, depleted  
 and chemically buoyant „cold nose,, of the mantle  
 wedge.
- In conclusion, despite recent progress in both  
 observation and modelling many of the first-order  
 features of intra-oceanic subduction remain only  
 partly known and require further cross-disciplinary  
 efforts.
- Acknowledgements** This work was supported by ETH  
 Research Grants ETH-0807-2, ETH-0807-3, ETH-0609-2,  
 SNF Research Grants 200020-126832, 200020-129487, SNF  
 ProDoc program 4-D-Adamello and TopoEurope Program.

## References

- Abbott RN, Draper G, Broman BN (2006) P-T path for ultra-  
 high-pressure garnet ultramafic rocks of the Cuaba Gneiss,  
 Rio San Juan complex, Dominican Republic. *Int Geol Rev*  
 48:778–790
- Afonso JC, Ranalli G, Fernandez M (2007) Density structure  
 and buoyancy of the oceanic lithosphere revisited. *Geophy*  
*Res Lett* 34, Article Number: L10302
- Afonso JC, Zlotnik S, Fernandez M (2008) Effects of composi-  
 tional and rheological stratifications on small-scale convec-  
 tion under the oceans: implications for the thickness of  
 oceanic lithosphere and seafloor flattening. *Geophys Res*  
*Lett* 35, Article Number: L20308
- Alvarez-Marron J, Perez-Estaun A, Danobeitia JJ, Pulgar JA,  
 Martinez Catalan JR, Marcos A, Bastida E, Ayarza Arribas  
 R, Aller J, Gallart A, Gonzalez-Lodeiro E, Banda E, Comas

1238 [AU7](#)

- 1254 MC, Cordoba D (1996) Seismic structure of the northern  
1255 continental margin of Spain from ESCIN deep seismic pro-  
1256 files. *Tectonophysics* 264:153–174
- 1257 Alvarez-Marron J, Rubio E, Torne M (1997) Subduction-related  
1258 structures in the North Iberian Margin. *J Geophys Res*  
1259 102:22497–22511
- 1260 Arai S, Ishimaru S (2008) Insights into petrological char-  
1261 acteristics of the lithosphere of mantle wedge beneath  
1262 arcs through peridotite xenoliths: a review. *J Petrol*  
1263 49:665–695
- 1264 Arcay D, Tric E, Doin MP (2005) Numerical simulations of  
1265 subduction zones: effect of slab dehydration on the mantle  
1266 wedge dynamics. *Phys Earth Planet Inter* 149:133–153
- 1267 Arculus RJ, Johnson RW (1981) Island-arc magma sources: a  
1268 geochemical assessment of the roles of slab derived compo-  
1269 nents and crustal contamination. *Geochem J* 15:109–133
- 1270 Billen M, Gurnis M (2001) A low viscosity wedge in subduction  
1271 zones. *Earth Planet Sci Lett* 193:227–236
- 1272 Bourdon B, Turner S, Dosseto A (2003) Dehydration and partial  
1273 melting in subduction zones: constraints from U-series dis-  
1274 equilibria. *J Geophys Res* 108, Article Number: 2291
- 1275 Boyd OS, Jones CH, Sheehan AF (2004) Foundering lithosphere  
1276 imaged beneath the southern Sierra Nevada, California,  
1277 USA. *Science* 305:660–662
- 1278 Burg JP (2011) The Asia-Kohistan-India collision. Review and  
1279 discussion. In: Brown D, Ryan P (eds) *Arc-continent colli-*  
1280 *sion: the making of an orogen*, *Frontiers in earth sciences*.  
1281 Springer, Heidelberg
- 1282 Burg J-P, Bodinier J-L, Gerya T, Bedini R-M, Boudier F,  
1283 Dautria J-M, Prikhodko V, Efimov A, Pupier E, Balanec J-L  
1284 (2009) Translithospheric mantle diapirism: geological evi-  
1285 dence and numerical modelling of the Kondyor zoned ultra-  
1286 mafic complex (Russian Far-East). *J Petrol* 50:289–321
- 1287 Calvert AJ (2011) The seismic structure of island arc crust.  
1288 In: Brown D, Ryan P (eds) *Arc-continent collision: the*  
1289 *making of an orogen*, *Frontiers in earth sciences*. Springer,  
1290 Heidelberg
- 1291 Casey JF, Dewey JF (1984) Initiation of subduction zones along  
1292 transforms and accreting plate boundaries, triple junction  
1293 evolution, and forearc spreading centers: implications for  
1294 ophiolitic geology and obduction. In: Gass IG, Lippard SJ,  
1295 Shelton AW (eds) *Ophiolites and oceanic lithosphere*, vol  
1296 13. *Geol Soc Spec Publ*, London, pp 269–290
- 1297 Castro A, Gerya TV (2008) Magmatic implications of mantle  
1298 wedge plumes: experimental study. *Lithos* 103:138–148
- 1299 Castro A, García-Casco A, Fernández C, Corretgé LG, Moreno-  
1300 Ventas I, Gerya T, Löw I (2009) Ordovician ferrosilicic  
1301 magmas: experimental evidence for ultrahigh temperatures  
1302 affecting a metagreywacke source. *Gondwana Res*  
1303 16:622–632
- 1304 Castro A, Gerya T, Garcia-Casco A, Fernandez C, Diaz-  
1305 Alvarado J, Moreno-Ventas I, Low I (2010) Melting rela-  
1306 tions of MORB-sediment melanges in underplated mantle  
1307 wedge plumes; implications for the origin of Cordilleran-  
1308 type batholiths. *J Petrol* 51:1267–1295
- 1309 Churikova T, Dorendorf F, Worner G (2001) Sources and fluids  
1310 in the mantle wedge below Kamchatka, evidence from  
1311 across-arc geochemical variation. *J Petrol* 42:1567–1593
- 1312 Cloetingh SAPL, Wortel MJR, Vlaar NJ (1982) Evolution of  
1313 passive continental margins and initiation of subduction  
1314 zones. *Nature* 297:139–142
- Cloos M (1982) Flow melanges: numerical modelling and geo- 1315  
logic constraints on their origin in the Franciscan subduction 1316  
complex, California. *Geol Soc Am Bull* 93:330–345 1317
- Cloos M (1993) Lithospheric buoyancy and collisional orogen- 1318  
esis: subduction of oceanic plateaus, continental margins, 1319  
island arcs, spreading ridges, and seamounts. *Geol Soc Am* 1320  
*Bull* 105:715–737 1321
- Cloos M, Shreve RL (1988a) Subduction-channel model of 1322  
prism accretion, melange formation, sediment subduction, 1323  
and subduction erosion at convergent plate margins, 1, Back- 1324  
ground and description. *Pure Appl Geophys* 128:455–500 1325
- Cloos M, Shreve RL (1988b) Subduction-channel model of 1326  
prism accretion, melange formation, sediment subduction, 1327  
and subduction erosion at convergent plate margins, 2, Impli- 1328  
cations and discussion. *Pure App Geophys* 128:501–545 1329
- Collins WJ (2003) Slab pull, mantle convection, and Pangae- 1330  
an assembly and dispersal. *Earth Planet Sci Lett* 205:225–237 1331
- Conder JA, Wiens DA (2007) Rapid mantle flow beneath the 1332  
Tonga volcanic arc. *Earth Planet Sci Lett* 264:299–307 1333
- Conrad WK, Kay RW (1984) Ultramafic and mafic inclusions 1334  
from Adak Island; crystallization history, and implications 1335  
for the nature of primary magmas and crustal evolution in the 1336  
Aleutian arc. *J Petrol* 25:88–125 1337
- Davidson JP (1996) Deciphering mantle and crustal signatures 1338  
in subduction zone magmatism. In: Bebout GE, Scholl DW,  
Kirby SH, Platt JR (eds) *Subduction top to bottom*. *Ameri-* 1339  
*can Geophysical Union Monographs*, vol 96., pp 251–262 1340
- Davies GF (1999) *Dynamic Earth*. Cambridge University Press, 1342  
New York 1343
- Davies JH, Stevenson DJ (1992) Physical model of source 1344  
region of subduction zone volcanics. *J Geophys Res* 1345  
97:2037–2070 1346
- Defant MJ, Drummond MS (1990) Derivation of some modern 1347  
arc magmas by melting of young subducted lithosphere. 1348  
*Nature* 347:662–665 1349
- Dewey JF (1969) Continental margins: a model for conversion 1350  
of Atlantic type to Andean type. *Earth Planet Sci Lett* 1351  
6:189–197 1352
- Dickinson WR, Seely DR (1979) Structure and stratigraphy of 1353  
fore-arc regions. *Am Assoc Petrol Geol Bull* 63:2–31 1354
- Dimalanta C, Taira A, Yumul GP, Tokuyama H, Mochizuki K 1355  
(2002) New rates of western Pacific island arc magmatism 1356  
from seismic and gravity data. *Earth Planet Sci Lett* 1357  
202:105–115 1358
- Doin M-P, Henry P (2001) Subduction initiation and continental 1359  
crust recycling: the roles of rheology and eclogitization. 1360  
*Tectonophysics* 342:163–191 1361
- Dosseto A, Bourdon B, Joron J-L, Dupre B (2003) U-Th-Pa-Ra 1362  
study of the Kamchatka arc: new constraints on the genesis 1363  
of arc lavas. *Geochem Cosmochem Acta* 67:2857–2877 1364
- Eiler JM, Carr MJ, Reagan M, Stolper EM (2005) Oxygen 1365  
isotope constraints on the sources of Central American 1366  
arc lavas. *Geochem Geophys Geosyst* 6, Article Number: 1367  
Q07007 1368
- Eiler JM, Schiano P, Valley JM, Kita NT, Stolper EM (2007) 1369  
Oxygen-isotope and trace element constraints on the origins 1370  
of silica-rich melts in the subarc mantle. *Geochem Geophys* 1371  
*Geosyst* 8, Article Number: Q09012 1372
- Elliott T (2003) Tracers of the slab. In: Eiler J (ed) *Inside* 1373  
*the subduction factory*. American Geophysical Union, 1374  
Washington, DC, pp 23–46 1375

- 1376 Elliott T, Plank T, Zindler A, White W, Bourdon B (1997) 1436  
 1377 Element transport from slab to volcanic front at the Mariana 1437  
 1378 arc. *J Geophys Res* 102:14991–15019 1438
- 1379 Erickson SG (1993) Sedimentary loading, lithospheric flexure, 1439  
 1380 and subduction initiation at passive margins. *Geology* 1440  
 1381 21:125–128 1441
- 1382 Ernst WG (1977) Mineral parageneses and plate tectonic set- 1442  
 1383 tings of relatively high-pressure metamorphic belts. *Fortschr* 1443  
 1384 *Miner* 54:192–222 1444
- 1385 Federico L, Crispini L, Scambelluri M, Capponi G (2007) 1445  
 1386 Ophiolite mélange zone records exhumation in a fossil sub- 1446  
 1387 duction channel. *Geology* 35:499–502 1447
- 1388 Fyfe WS, Leonardos OH (1977) Speculations on causes of 1448  
 1389 crustal rifting and subduction, with applications to Atlantic 1449  
 1390 margin of Brazil. *Tectonophysics* 42(1):29–36 1450
- 1391 George R, Turner S, Hawkesworth C, Morris J, Nye C, Ryan J, 1451  
 1392 Zheng S-H (2003) Melting processes and fluid and sediment 1452  
 1393 transport rates along the Alaska-Aleutian arc from an 1453  
 1394 integrated U-Th-Ra-Be isotope study. *J Geophys Res* 108, 1454  
 1395 doi:10.1029/2002JB001916 1455
- 1396 Gerya TV, Burg J-P (2007) Intrusion of ultramafic magmatic 1456  
 1397 bodies into the continental crust: numerical simulation. *PEPI* 1457  
 1398 160:124–142 1458
- AUB 1399 Gerya TV, Meilick FI (2010) Geodynamic regimes of subduc- 1459  
 1400 tion under an active margin: effects of rheological weaken- 1460  
 1401 ing by fluids and melts. *J Metamorphic Geol* (submitted) 1461
- 1402 Gerya TV, Yuen DA (2003) Rayleigh-Taylor instabilities from 1462  
 1403 hydration and melting propel "cold plumes" at subduction 1463  
 1404 zones. *Earth Planet Sci Lett* 212:47–62 1464
- 1405 Gerya TV, Stoeckert B, Perchuk AL (2002) Exhumation of 1465  
 1406 high-pressure metamorphic rocks in a subduction channel – 1466  
 1407 a numerical simulation. *Tectonics* 21, Article Number: 1056 1467
- 1408 Gerya TV, Yuen DA, Sevre EOD (2004) Dynamical causes for 1468  
 1409 incipient magma chambers above slabs. *Geology* 32:89–92 1469
- 1410 Gerya TV, Connolly JAD, Yuen DA, Górczyk W, Capel AM 1470  
 1411 (2006) Seismic implications of mantle wedge plumes. *Phys* 1471  
 1412 *Earth Planet Inter* 156:59–74 1472
- 1413 Gerya TV, Connolly JAD, Yuen DA (2008) Why is terrestrial 1473  
 1414 subduction one-sided? *Geology* 36:43–46 1474
- 1415 Górczyk W, Gerya TV, Connolly JAD, Yuen DA, Rudolph M 1475  
 1416 (2006) Large-scale rigid-body rotation in the mantle wedge 1476  
 1417 and its implications for seismic tomography. *Geochem Geo-* 1477  
 1418 *phys Geosyst* 7, Article Number: Q05018 1478
- 1419 Górczyk W, Guillot S, Gerya TV, Hattori K (2007a) Asthen- 1479  
 1420 opheric upwelling, oceanic slab retreat, and exhumation of 1480  
 1421 UHP mantle rocks: insights from Greater Antilles. *Geophys* 1481  
 1422 *Res Lett* 34, Article Number: L21309 1482
- 1423 Górczyk W, Gerya TV, Connolly JAD, Yuen DA (2007b) 1483  
 1424 Growth and mixing dynamics of mantle wedge plumes. 1484  
 1425 *Geology* 35:587–590 1485
- 1426 Goren L, Aharonov E, Mulugeta G, Koyi HA, Mart Y (2008) 1486  
 1427 Ductile deformation of passive margins: a new mechanism 1487  
 1428 for subduction initiation. *J Geophys Res* 113, Article Num- 1488  
 1429 ber: B08411 1489
- 1430 Grove TL, Chatterjee N, Parman SW, Medard E (2006) The 1490  
 1431 influence of H<sub>2</sub>O on mantle wedge melting. *Earth Planet Sci* 1491  
 1432 *Lett* 249:74–89 1492
- 1433 Gurnis M, Hall C, Lavier L (2004) Evolving force balance 1493  
 1434 during incipient subduction. *Geochem Geophys Geosyst* 5, 1494  
 1435 Article Number Q07001 1495
- Hall PS, Kincaid C (2001) Diapiric flow at subduction zones: a 1436  
 recipe for rapid transport. *Science* 292:2472–2475 1437
- Hall C, Gurnis M, Sdrolias M, Lavier LL, Müller RD (2003) 1438  
 Catastrophic initiation of subduction following forced con- 1439  
 vergence across fracture zones, *Earth Planet. Sci Lett* 1440  
 212:15–30 1441
- Hauff F, Hoernle K, Schmidt A (2003) Sr-Nd-Pb composition of 1442  
 Mesozoic Pacific oceanic crust (Site 1149 and 801, ODP Leg 1443  
 185): implications for alteration of ocean crust and the input 1444  
 into the Izu-Bonin-Mariana subduction system. *Geochem* 1445  
*Geophys Geosyst* 4, Article Number: 8913 1446
- Hawkesworth CJ, Gallagher K, Hergt JM, McDermott F (1993) 1447  
 Trace element fractionation processes in the generation of 1448  
 island arc basalts. *Philos Trans R Soc London Ser A* 1449  
 342:179–191 1450
- Hawkesworth CJ, Turner SP, McDermott F, Peate DW, van 1451  
 Calsteren P (1997) U-Th isotopes in arc magmas: implica- 1452  
 tions for element transfer from the subducted crust. *Science* 1453  
 276:551–555 1454
- Hebert LB, Antoshechkina P, Asimow P, Gurnis M (2009) 1455  
 Emergence of a low-viscosity channel in subduction zones 1456  
 through the coupling of mantle flow and thermodynamics, 1457  
*Earth Planet. Sci Lett* 278:243–256 1458
- Hermann J, Muntener O, Scambelluri M (2000) The importance 1459  
 of serpentinite mylonites for subduction and exhumation of 1460  
 oceanic crust. *Tectonophysics* 327:225–238 1461
- Hilde TWE, Uyeda S, Kroenke L (1976) Evolution of 1462  
 the western Pacific and its margin. *Tectonophysics* 1463  
 38:145–165 1464
- Holbrook WS, Lizarralde D, McGeary S, Bangs N, Diebold J 1465  
 (1999) Structure and composition of Aleutian island arc 1466  
 and implications for continental crustal growth. *Geology* 1467  
 27:31–34 1468
- Honda S, Saito M (2003) Small-scale convection under the 1469  
 back-arc occurring in the low viscosity wedge, *Earth Planet.* 1470  
*Sci Lett* 216:703–715 1471
- Honda S, Yoshida T (2005) Application of the model of small- 1472  
 scale convection under the island arc to the NE Honshu 1473  
 subduction zone. *Geochem Geophys Geosyst* 6, Article 1474  
 Number: Q06004 1475
- Honda S, Saito M, Nakakuki T (2002) Possible existence of 1476  
 small-scale convection under the back arc. *Geophys Res Lett* 1477  
 29:20–43 1478
- Honda S, Yoshida T, Aoike K (2007) Spatial and temporal 1479  
 evolution of arc volcanism in the northeast Honshu and 1480  
 Izu-Bonin arcs: evidence of small-scale convection under 1481  
 the island arc? *Isl Arc* 16:214–223 1482
- Honda S, Gerya T, Zhu G (2010) A simple three-dimensional 1483  
 model of thermo-chemical convection in the mantle wedge. 1484  
*Earth Planet Sci Lett* 290:311–318 1485
- Hsu KJ (1971) Franciscan mélange as a model for eugeosuncl- 1486  
 inal sedimentation and underthrusting tectonics. *J Geophys* 1487  
*Res* 76:1162–1170 1488
- Ishikawa T, Nakamura E (1994) Origin of the slab component in 1489  
 arc lavas from across-arc variation of B and Pb isotopes. 1490  
*Nature* 370:205–208 1491
- Ishikawa T, Tera F (1999) Two isotopically distinct fluid com- 1492  
 ponents involved in the Mariana Arc: evidence from Nb/B 1493  
 ratios and B, Sr, Nd, and Pb isotope systematic. *Geology* 1494  
 27:83–86 1495

- 1496 Ishizuka O, Taylor RN, Milton JA, Nesbitt RW (2003) Fluid-  
1497 mantle interaction in an intra-oceanic arc: constraints  
1498 from high-precision Pb isotopes, *Earth Planet. Sci Lett*  
1499 211:221–236
- 1500 Ishizuka O, Taylor RN, Milton JA, Nesbitt RE, Yuasa M,  
1501 Sakamoto I (2006) Variation in the mantle sources of the  
1502 northern Izu arc with time and space – Constraints from  
1503 high-precision Pb isotopes. *J Volcanol Geotherm Res*  
1504 156:266–290
- 1505 Ito E, Stern RJ (1986) Oxygen-isotopic and strontium isotopic  
1506 investigations of subduction zone volcanism – the case of the  
1507 Volcano Arc and the Marianas Island-Arc. *Earth Planet Sci*  
1508 *Lett* 76:312–320
- 1509 Iwamori H (1998) Transportation of H<sub>2</sub>O and melting in sub-  
1510 duction zones, *Earth Planet. Sci Lett* 160:65–80
- 1511 Iwamori H (2007) Transportation of H<sub>2</sub>O beneath the Japan arcs  
1512 and its implications for global water circulation. *Chem Geol*  
1513 239:182–198
- 1514 Jagoutz O, Müntener O, Burg J-P, Ulmer P, Jagoutz E (2006)  
1515 Lower continental crust formation through focused flow in  
1516 km-scale melt conduits: the zoned ultramafic bodies of the  
1517 Chilas Complex in the Kohistan island arc (NW Pakistan).  
1518 *Earth Planet Sci Lett* 242:320–342
- 1519 Jull M, Kelemen PB (2001) On the conditions for lower crustal  
1520 convective instability, *J. Geophys. Res., B. Solid Earth Plan-*  
1521 *ets* 106:6423–6446
- 1522 Jung H, Karato S (2001) Water-induced fabric transitions in  
1523 olivine. *Science* 293:1460–1463
- 1524 Karig DE (1982) Initiation of subduction zones: implications for  
1525 arc evolution and ophiolite development. *Geol Soc Lond*  
1526 *Spec Pub* 10:563–576
- 1527 Karson J, Dewey JF (1978) Coastal Complex, western New-  
1528 foundland: an early Ordovician oceanic fracture zone. *Bull-*  
1529 *Geol Soc Amer* 89:1037–1049
- 1530 Kay SM, Kay RW (1985) Aleutian tholeiitic and calc-alkaline  
1531 magma series: 1. The mafic phenocrysts. *Contrib Mineral*  
1532 *Petrol* 90:276–290
- 1533 Kay SM, Kay RW (1991) Creation and destruction of lower  
1534 continental crust. In: Stoeckert B, Wedepohl KH (eds)  
1535 *Crustal dynamics, pathways and records*, International  
1536 *Journal of Earth Sciences*, vol 80, 2, Springer, Berlin,  
1537 pp 259–278
- 1538 Kay SM, Kay RW (1993) Delamination and delamination mag-  
1539 matism. In: Green AG, Kroener A, Goetze HJ, Pavlenkova N  
1540 (eds) *New horizons in strong motion; seismic studies*  
1541 *and engineering practice*, Tectonophysics, vol 219, 1–3,  
1542 Elsevier, Amsterdam, Netherlands, pp 177–189
- 1543 Kelemen PB, Hart SR, Bernstein S (1998) Silica enrichment in  
1544 the continental upper mantle via melt/rock reaction. *Earth*  
1545 *Planet Sci Lett* 164:387–406
- 1546 Kelemen P, Hanghoj K, Greene A (2003) One view of the  
1547 geochemistry of subduction-related magmatic arcs, with an  
1548 emphasis on primitive andesite and lower crust. In: Rudnick  
1549 RL (ed) *The crust, treatise on geochemistry*, vol 3. Elsevier  
1550 Pergamon, Oxford, pp 593–659
- 1551 Kelemen PB, Rilling JL, Parmentier EM, Mehl L, Hacker BR  
1552 (2004a) Thermal structure due to solid-state flow in the  
1553 mantle wedge beneath arcs. In: Eiler JM (ed) *Inside the*  
1554 *subduction factory*, vol 138, *Geophys Monogr Ser. AGU*,  
1555 Washington, DC, pp 293–311
- Kelemen PB, Yogodzinski GM, Scholl DW (2004b) Along-  
strike variation in the Aleutian island arc: genesis of high  
Mg# andesite and implications for continental crust. In: Eiler  
JM (ed) *Inside the subduction factory*, vol 138, *Geophys*  
*Monogr Ser. AGU*, Washington, DC, pp 223–276
- Kelley KA, Plank T, Grove TL, Stolper EM, Newman S, Hauri  
E (2006) Mantle melting as a function of water content  
beneath back-arc basins. *J Geophys Res* 111, Article Num-  
ber: B09208
- Kemp DV, Stevenson DJ (1996) A tensile, flexural model for the  
initiation of subduction. *Geophys J Int* 125:73–94
- Kessel R, Schmidt MW, Pettke T, Ulmer P (2005) The trace  
element signature of subduction zone fluids, melts, and  
supercritical liquids at 120–180 km depth. *Nature*  
437:724–727
- Kimura J-I, Stern RJ (2009) Neogene volcanism of the Japan  
island arc: the K-h relationship revisited. In: *Circum pacific*  
*tectonics, geologic evolution, and ore deposits*. Arizona  
*Geological Society Digest*, Arizona Geological Society,  
Tucson, vol 22, pp 187–202
- Kimura J, Yoshida T (2006) Contributions of slab fluid, mantle  
wedge and crust to the origin of quaternary lavas in the NE  
Japan arc. *J Petrol* 47:2185–2232
- Kimura J-I, Stern RJ, Yoshida T (2005) Re-initiation of subduc-  
tion and magmatic responses in SW Japan during Neogene  
time. *Geol Soc Am Bull* 117:969–986
- Kimura J-I, Hacker B.R, van Keken PE, Kawabata H, Yoshida T,  
Stern RJ (2009) Arc basalt simulator version 2, a simulation  
for slab dehydration and fluid-fluxed mantle melting for arc  
basalts: modeling scheme and application. *Geochem Geoph-*  
*ys Geosyst* 10, Article Number: Q09004
- Kodaira S, Sato T, Takahashi N, Ito A, Tamura Y, Tatsumi Y,  
Kaneda Y (2006) Seismological evidence for variable  
growth of crust along the Izu intraoceanic arc. *J Geophys*  
*Res* 112, Article Number: B05104
- Kodaira S, Sato T, Takahashi N, Miura S, Tamura Y, Tatsumi Y,  
Kaneda Y (2007) New seismological constraints on growth  
of continental crust in the Izu-Bonin intra-oceanic arc.  
*Geology* 35:1031–1034
- Kodaira S, Sato T, Takahashi N, Yamashita M, No T, Kaneda Y  
(2008) Seismic imaging of a possible paleoarc in the Izu-  
Bonin intraoceanic arc and its implications for arc evolution  
processes. *Geochem Geophys Geosyst* 9, Article Number:  
Q10X01
- Krebs M, Maresch WV, Schertl H-P, Münker C, Baumann A,  
Draper G, Idleman B, Trapp E (2008) The dynamics of  
intra-oceanic subduction zones: a direct comparison  
between fossil petrological evidence (Rio San Juan Com-  
plex, Dominican Republic) and numerical simulation. *Lithos*  
103:106–137
- Kushiro I, Syono Y, Akimoto S (1968) Melting of a peridotite  
nodule at high pressures and high water pressures. *J Geophys*  
*Res* 73:6023–6029
- Leat PT, Larter RD (2003) Intra-oceanic subduction systems:  
introduction. In: Larter RD, Leat PT (eds) *Intra-oceanic*  
*subduction systems: tectonic and magmatic processes*, vol  
219. *Geological Society of London, Special Publications*,  
London, pp 1–17
- Leat PT, Riley TR, Wareham CD, Millar IL, Kelley SP, Storey  
BC (2002) Tectonic setting of primitive magmas in volcanic

- 1616 arcs: an example from the Antarctic Peninsula. *J Geol Soc*  
1617 *Lond* 159:31–44
- 1618 Manea VC, Manea M, Kostoglodov V, Sewell G (2005)  
1619 Thermo-mechanical model of the mantle wedge in Central  
1620 Mexican subduction zone and a blob tracing approach for the  
1621 magma transport. *Phys Earth Planet Inter* 149:165–186
- 1622 Manning CE (2004) The chemistry of subduction-zone fluids.  
1623 *Earth Planet Sci Lett* 223:1–16
- 1624 Marques FO, Gerya T, Nikolaeva K (2008) Subduction initiation  
1625 at a passive margin: a prototype candidate. 33rd IGC,  
1626 Abstract Volume, Oslo, Norway
- 1627 Mart Y, Aharonov E, Mulugeta G, Ryan W, Tentler T, Goren L  
1628 (2005) Analogue modelling of the initiation of subduction.  
1629 *Geophys J Int* 160:1081–1091
- 1630 Martin H (1999) Adakitic magmas: modern analogues of  
1631 Archaean granitoids. *Lithos* 46:411–429
- 1632 Martin H, Smithies RH, Rapp R, Moyen J-F, Champion D  
1633 (2005) An overview of adakite, tonalite-trondhjemite-grano-  
1634 diorite (TTG), and sanukitoid: relationships and some impli-  
1635 cations for crustal evolution. *Lithos* 79:1–24
- 1636 Maruyama S, Liou JG, Terabayashi M (1996) Blueschists and  
1637 eclogites in the world and their exhumation. *Int Geol Rev*  
1638 38:485–594
- 1639 Masson DG, Cartwright JA, Pinheiro LM, Whitmarsh RB,  
1640 Beslier M-O, Roeser H (1994) Compressional deformation  
1641 at the ocean–continent transition in the NE Atlantic. *J Geol*  
1642 *Soc London* 151:607–613
- 1643 McCulloch MT, Gamble JA (1991) Geochemical and geodyna-  
1644 mical constraints on subduction zone magmatism. *Earth*  
1645 *Planet Sci Lett* 102:358–374
- 1646 McKenzie DP (1977) The initiation of trenches: a finite ampli-  
1647 tude instability. In: Talwani M, Pitman WC III (eds) *Island*  
1648 *arcs, deep sea trenches and back-arc basins*, vol 1, Maurice  
1649 *Ewing Series*. AGU, Washington, DC, pp 57–61
- 1650 Mitchell AHG (1984) Initiation of subduction of post-collision  
1651 foreland thrusting and back-thrusting. *J Geodyn* 1:103–120
- 1652 Moriguti T, Shibata T, Nakamura E (2004) Lithium, boron and  
1653 lead isotope and trace element systematics of Quaternary  
1654 basaltic volcanic rocks in northeastern Japan: mineralogical  
1655 controls on slab-derived fluid composition. *Chem Geol*  
1656 212:81–100
- 1657 Müller S, Phillips RJ (1991) On the initiation of subduction.  
1658 *J Geophys Res* 96:651–665
- 1659 Müntener O, Kelemen PB, Grove TL (2001) The role of H<sub>2</sub>O  
1660 during crystallization of primitive arc magmas under upper-  
1661 most mantle conditions and genesis of igneous pyroxenites;  
1662 an experimental study. *Contrib Mineral Petrol* 141:643–658
- 1663 Nakajima J, Hasegawa A (2003a) Estimation of thermal struc-  
1664 ture in the mantle wedge of northeastern Japan from seismic  
1665 attenuation data. *Geophys Res Lett* 30, Article Number:  
1666 1760
- 1667 Nakajima J, Hasegawa A (2003b) Tomographic imaging of  
1668 seismic velocity structure in and around the Onikobe volca-  
1669 nic area, northeastern Japan: implications for fluid distribu-  
1670 tion. *J Volcanol Geotherm Res* 127:1–18
- 1671 Nikolaeva K, Gerya TV, Connolly JAD (2008) Numerical mod-  
1672 elling of crustal growth in intraoceanic volcanic arcs. *Phys*  
1673 *Earth Planet Inter* 171:336–356
- 1674 Nikolaeva K, Gerya TV, Marques FO (2010) Subduction initia-  
1675 tion at passive margins: numerical modeling. *J Geophys Res*  
1676 115, Article Number: B03406
- Niu Y, O'Hara MJ, Pearce JA (2003) Initiation of subduction  
1677 zones as a consequence of lateral compositional buoyancy  
1678 contrast within the lithosphere: a petrological perspective.  
1679 *J Petrol* 44(5):851–866
- 1680 Obata M, Takazawa E (2004) Compositional continuity and  
1681 discontinuity in the Horoman peridotite, Japan, and its impli-  
1682 cation for melt extraction processes in partially molten upper  
1683 mantle. *J Petrol* 45:223–234
- 1684 Oxburg ER, Parmentier EM (1977) Compositional and density  
1685 stratification in oceanic lithosphere – causes and conse-  
1686 quences. *J Geol Soc London* 133:343–355
- 1687 Pascal C, Cloetingh SAPL (2009) Gravitational potential stresses  
1688 and stress field of passive continental margins: insights from  
1689 the south-Norway shelf. *Earth Planet Sci Lett* 277:464–473
- 1690 Peacock SM, Wang K (1999) Seismic consequence of warm  
1691 versus cool subduction metamorphism: examples from  
1692 southwest and northeast Japan. *Science* 286:937–939
- 1693 Pearce JA, Peate DW (1995) Tectonic implications of the com-  
1694 position of volcanic arc magmas. *Annu Rev Earth Planet Sci*  
1695 23:251–285
- 1696 Pearce JA, Stern RJ, Bloomer SH, Fryer P (2005) Geochemical  
1697 mapping of the Mariana arc-basin system: implications for  
1698 the nature and distribution of subduction components. *Geo-*  
1699 *chem Geophys Geosyst* 6, Article Number: Q07006
- 1700 Pichavant M, Macdonald R (2003) Mantle genesis and crustal  
1701 evolution of primitive calc-alkaline basaltic liquids from  
1702 the Lesser Antilles arc. In: Larter RD, Leat PT (eds)  
1703 *Intra-oceanic Subduction Systems: Tectonic and Magmatic*  
1704 *Processes*, vol 219. Geological Society of London, Special  
1705 *Publications*, London, pp 239–254
- 1706 Plank T, Langmuir CH (1993) Tracing trace-elements from  
1707 sediment input to volcanic output at Subduction Zones.  
1708 *Nature* 362:739–743
- 1709 Platt JP (1993) Exhumation of high-pressure rocks: a review of  
1710 concepts and processes. *Terra Nova* 5:119–133
- 1711 Poli S, Schmidt MW (1995) H<sub>2</sub>O transport and release in  
1712 subduction zones: experimental constraints on basaltic and  
1713 andesitic systems. *J Geophys Res* 100:22299–22314
- 1714 Poli S, Schmidt MW (2002) Petrology of subducted slabs. *Annu*  
1715 *Rev Earth Planet Sci* 30:207–235
- 1716 Pysklywec RN, Mitrovica JX, Ishii M (2003) Mantle avalanche  
1717 as a driving force for tectonic reorganization in the south-  
1718 west Pacific. *Earth Planet Sci Lett* 209:29–38
- 1719 Rapp EP, Watson EB (1995) Dehydration melting of metabasalt  
1720 at 8–32 kbar: implications for continental growth and  
1721 crustal-mantle recycling. *J Petrol* 36:891–931
- 1722 Regenauer-Lieb K, Yuen DA, Branlund J (2001) The initiation  
1723 of subduction: critically by addition of water? *Science*  
1724 294:578–580
- 1725 Reymer A, Schubert G (1984) Phanerozoic addition rates to the  
1726 continental crust and crustal growth. *Tectonics* 3:63–77
- 1727 Ring U, Brandon MT, Willett SD, Lister GS (1999) Ring U,  
1728 Brandon MT, Lister GS, Willett SD (eds) Exhumation pro-  
1729 cesses: normal faulting, ductile flow, and erosion, Geologi-  
1730 cal Society, Special Publication, vol 154, pp 1–27
- 1731 Rudnick RL, Gao S (2003) The composition of the continental  
1732 crust. In: Rudnick RL (ed) *The crust, treatise on geochemis-*  
1733 *try*, vol 3. Elsevier, Oxford, pp 1–64
- 1734 Ryan JG, Morris J, Tera F, Leeman WP, Tsvetkov A (1995)  
1735 Cross-arc geochemical variations in the Kurile Arc as a  
1736 function of slab depth. *Science* 270:625–627
- 1737

- 1738 Sajona FG, Maury RC, Bellon H, Cotten J, Defant M (1996) 1800  
 1739 High field strength element enrichment of Pliocene-Pleisto- 1801  
 1740 cene island arc basalts, Zamboanga Peninsula, western 1802  
 1741 Mindanao (Philippines). *J Petrol* 37:693–726 1803  
 1742 Sajona FG, Maury RC, Prouteau G, Cotten J, Schiano P, 1804  
 1743 Bellon H, Fontaine L (2000) Slab melt as metasomatic 1805  
 1744 agent in island arc magma mantle sources, Negros and 1806  
 1745 Batan (Philippines). *Isl Arc* 9:472–486 1807  
 1746 Schellart WP, Freeman J, Stegman DR, Moresi L, May D (2007) 1808  
 1747 Evolution and diversity of subduction zones controlled by 1809  
 1748 slab width. *Nature* 446:308 1810  
 1749 Schmidt MW, Poli S (1998) Experimentally based water bud- 1811  
 1750 gets for dehydrating slabs and consequences for arc magma 1812  
 1751 generation. *Earth Planet Sci Lett* 163:361–379 1813  
 1752 Shibata T, Nakamura E (1997) Across-arc variations of isotope 1814  
 1753 and trace element compositions from Quaternary basaltic 1815  
 1754 rocks in northeastern Japan: implications for interaction 1816  
 1755 between subducted oceanic slab and mantle wedge. *J Geophy- 1817  
 1756 s Res* 102:8051–8064 1818  
 1757 Shimoda G, Nohda S (1995) Lead isotope analyses: an application 1819  
 1758 to GSJ standard rock samples. *Human Environ Stud* 4:29–36 1820  
 1759 Shreve RL, Cloos M (1986) Dynamics of sediment subduction, 1821  
 1760 melange formation, and prism accretion. *J Geophys Res* 1822  
 1761 91:10229–10245 1823  
 1762 Sizova E, Gerya T, Brown M, Perchuk LL (2009) Subduction 1824  
 1763 styles in the Precambrian: insight from numerical experi- 1825  
 1764 ments. *Lithos*. doi:10.1016/j.lithos.2009.05.028 1826  
 1765 Smith IEM, Worthington TJ, Price RC, Gamble JA (1997) Primi- 1827  
 1766 tive magmas in arc-type volcanic associations: examples from 1828  
 1767 the southwest Pacific. *Can Mineral* 35:257–273 1829  
 1768 Solomatov VS (2004) Initiation of subduction by small-scale 1830  
 1769 convection. *J Geophys Res* 109, Article Number: B05408 1831  
 1770 Stern RJ (2002) Subduction zones. *Rev Geophys* 40:3-1–3-38 1832  
 1771 Stern RJ (2004) Subduction initiation: spontaneous and induced. 1833  
 1772 *Earth Planet Sci Lett* 226:275–292 1834  
 1773 Stern RJ, Bloomer SH (1992) Subduction zone infancy: exam- 1835  
 1774 ples from the Eocene Izu-Bonin-Mariana and Jurassic Cali- 1836  
 1775 fornia arcs. *Geol Soc Am Bull* 104:1621–1636 1837  
 1776 Stern RJ, Fouch MJ, Klemperer SL (2003) An overview of the 1838  
 1777 Izu-Bonin-Mariana subduction factory. In: Eiler J (ed) *Inside 1839  
 1778 the subduction factory*, vol 138, *Geophys Monogr Ser. AGU,*  
 1779 Washington, DC, pp 175–222 1840  
 1780 Stolper E, Newman S (1994) The role of water in the petrogen- 1841  
 1781 esis of Mariana trough magmas, *Earth Planet. Sci Lett* 1842  
 1782 121:293–325 1843  
 1783 Straub SM, Layne GD (2003) The systematic of chlorine, fluo- 1844  
 1784 rine, and water in Izu arc front volcanic rocks: implications 1845  
 1785 for volatile recycling in subduction zones. *Geochim Cosmo- 1846  
 1786 chim Acta* 67:4179–4203 1847  
 1787 Straub SM, LaGatta AB, Martin-DelPozzo AL, Langmuir CH 1848  
 1788 (2008) Evidence from high-Ni olivines for a hybridized 1849  
 1789 peridotite/pyroxenite source for orogenic andesites from 1850  
 1790 the central Mexican Volcanic Belt. *Geochim Geophys Geo- 1851  
 1791 syst* 9, Article Number: Q03007 1852  
 1792 Taira A, Saito S, Aoiike K, Morita S, Tokuyama H, Suyehiro K, 1853  
 1793 Takahashi N, Shinohara M, Kiyokawa S, Naka J, Klaus A 1854  
 1794 (1998) Nature and growth rate of the Northern Izu-Bonin 1855  
 1795 (Ogasawara) arc crust and their implications for continental 1856  
 1796 crust formation. *Isl Arc* 7:395–407 1857  
 1797 Takahashi N, Kodaira S, Klemperer SL, Tatsumi Y, Kaneda Y, 1858  
 1798 Suyehiro K (2007) Crustal structure and evolution of the 1859  
 1799 Mariana intra-oceanic island arc. *Geology* 35:203–206 1860  
 Takahashi N, Kodaira S, Tatsumi Y, Yamashita M, Sato T, 1800  
 Kaiho Y, Miura S, No T, Takizawa K, Kaneda Y (2009) 1801  
 Structural variations of arc crusts and rifted margins in the 1802  
 southern Izu-Ogasawara arc-back arc system. *Geochem 1803  
 Geophys Geosyst* 10, Article Number: Q09X08 1804  
 Tamura Y (1994) Genesis of island arc magmas by mantle 1805  
 derived bimodal magmatism: evidence from the Shirahama 1806  
 Group. *Jpn: J Petrol* 35:619–645 1807  
 Tamura Y, Tatsumi Y, Zhao DP, Kido Y, Shukuno H (2002) Hot 1808  
 fingers in the mantle wedge: new insights into magma gene- 1809  
 sis in subduction zones. *Earth Planet Sci Lett* 197:105–116 1810  
 Tatsumi Y, Eggins S (1995) Subduction-zone magmatism. 1811  
 Blackwell Science, Cambridge, MA, 211 pp 1812  
 Tatsumi Y, Hanyu T (2003) Geochemical modeling of dehydrat- 1813  
 ion and partial melting of subducting lithosphere: toward a 1814  
 comprehensive understanding of high-Mg andesite forma- 1815  
 tion in the Setouchi volcanic belt, SW Japan. *Geochem 1816  
 Geophys Geosyst* 4, Article Number: 1081 1817  
 Tatsumi Y, Stern RJ (2006) Manufacturing continental crust in 1818  
 the subduction factory. *Oceanography* 19:104–112 1819  
 Tatsumi Y, Shukuno H, Tani K, Takahashi N, Kodaira S, 1820  
 Kogiso T (2008) Structure and growth of the Izu-Bonin- 1821  
 Mariana arc crust: 2. Role of crust-mantle transformation 1822  
 and the transparent Moho in arc crust evolution. *J Geophys 1823  
 Res* 113, Article Number: B02203 1824  
 Taylor B, Martinez F (2003) Back-arc basin basalt systematic. 1825  
*Earth Planet Sci Lett* 210:481–497 1826  
 Toth J, Gurnis M (1998) Dynamics of subduction initiation at 1827  
 pre-existing fault zones. *J Geophys Res* 103:18053–18067 1828  
 Tsuchiya N, Suzuki S, Kimura J-I, Kagami H (2005) Evidence 1829  
 for slabmelt/mantle reaction: petrogenesis of Early Creta- 1830  
 ceous and Eocene high-Mg andesites from the Kitakami 1831  
 Mountains, Japan. *Lithos* 79:179–206 1832  
 Turner S, Foden J (2001) U, Th and Ra disequilibria, Sr, Nd, and 1833  
 Pb isotope and trace element variations in Sunda arc lavas: 1834  
 predominance of a subducted sediment component. *Contrib 1835  
 Mineral Petrol* 142:43–57 1836  
 Turner S, Hawkesworth C (1997) Constraints on flux rates and 1837  
 mantle dynamics beneath island arcs from Tonga-Kermadec 1838  
 lava geochemistry. *Nature* 389:568–573 1839  
 Turner S, Hawkesworth CJ, Rogers N, Bartlett J, Worthington 1840  
 T, Hergt J, Pearce JA, Smith IME (1997) 238U-230Th dis- 1841  
 equilibria, magma petrogenesis, and flux rates beneath the 1842  
 depleted Tonga-Kermadec island arc. *Geochim Cosmochim 1843  
 Acta* 61:4855–4884 1844  
 Ueda K, Gerya T, Sobolev SV (2008) Subduction initiation 1845  
 by thermal-chemical plumes. *Phys Earth Planet Inter* 1846  
 171:296–312 1847  
 Uyeda S, Ben-Avraham Z (1972) Origin and development of the 1848  
 Philippine Sea. *Nature* 240:176–178 1849  
 Van der Lee S, Regenauer-Lieb K, Yuen DA (2008) The role of 1850  
 water in connecting past and future episodes of subduction. 1851  
*Earth planet Sci Lett* 273:15–27 1852  
 Van Keken PE, King SD (2005) Thermal structure and dynam- 1853  
 ics of subduction zones: insights from observations and 1854  
 modeling. *Phys Earth Planet Inter* 149:1–6 1855  
 van Keken PE, Kiefer B, Peacock SM (2002) High resolution 1856  
 models of subduction zones: implications for mineral dehy- 1857  
 dration reactions and the transport of water into the deep 1858  
 mantle. *Geochim Geophys Geosyst* 3, Article Number: 1056 1859  
 Vlaar NJ, Wortel MJR (1976) Lithospheric aging, instability and 1860  
 subduction. *Tectonophysics* 32:331–351 1861

- 1862 Wyss M, Hasegawa A, Nakajima J (2001) Source and path of  
1863 magma for volcanoes in the subduction zone of northeastern  
1864 Japan. *Geophys Res Lett* 28:1819–1822
- 1865 Yogodzinski GM, Volynets ON, Koloskov AV, Seliverstov NI,  
1866 Matvenkov VV (1994) Magnesian andesites and the subduc-  
1867 tion component in a strongly calcalkaline series at the Pip  
1868 volcano, far Western Aleutian. *J Petrol* 35:163–204
- 1869 Yogodzinski GM, Lees JM, Churikova TG, Dorendorf F,  
1870 Woerner G, Volynets ON (2001) Geochemical evidence  
1871 for the melting of subducting oceanic lithosphere at plate  
1872 edges. *Nature* 409:500–504
- 1873 Zack T, Foley SF, Rivers T (2002) Equilibrium and disequilib-  
1874 rium trace element partitioning in hydrous eclogites  
1875 (Trescolmen, central Alps). *J Petrol* 43:1947–1974
- 1876 Zandt G, Gilbert H, Owens TJ, Ducea M, Saleeby J, Jones CH  
1877 (2004) Active foundering of a continental arc root beneath  
the southern Sierra Nevada in California. *Nature (Lond)* 431:41–46
- Zhao DP (2001) Seismological structure of subduction zones  
and its implications for arc magmatism and dynamics. *Phys  
Earth Planet Inter* 127:197–214
- Zhao DP, Hasegawa A, Horiuchi S (1992) Tomographic imag-  
ing of P and S wave velocity structure beneath north-eastern  
Japan. *J Geophys Res* 97:19909–19928
- Zhao DP, Mishra OP, Sanda R (2002) Influence of fluids and  
magma on earthquakes: seismological evidence. *Phys Earth  
Planet Inter* 132:249–267
- Zhu G, Gerya TV, Yuen DA, Honda S, Yoshida T, Connolly  
JAD (2009) 3-D Dynamics of hydrous thermalchemical  
plumes in oceanic subduction zones. *Geochem Geophys  
Geosyst* 10, Article Number Q11006

UNCORRECTED PROOF

# Author Queries

Chapter No.: 2

Query Refs.	Details Required	Author's response
AU1	"Zhu et al. 2008" is cited in text but not given in the reference list. Please provide details in the list or delete the citation from the text.	
AU2	"Stern et al. 2004" is cited in text but not given in the reference list. Please provide details in the list or delete the citation from the text.	
AU3	"Jagoutz et al. (2007)" is cited in text but not given in the reference list. Please provide details in the list or delete the citation from the text.	
AU4	The citation "Obata and Takazawa, 2003" (original) has been changed to "Obata and Takazawa 2004". Please check if appropriate.	
AU5	"Yogodzinski 2001" is cited in text but not given in the reference list. Please provide details in the list or delete the citation from the text.	
AU6	The citation "McCulloch, 1991" (original) has been changed to "McCulloch and Gamble 1991". Please check if appropriate.	
AU7	Please check reference "Poli and Schmidt 2002" was not cited in text.	
AU8	Please provide volume number and Pagination details for ref. Gerya and Meilick 2010.	
AU9	Please provide complete details for the ref. Ring et al. 1999.	